U.S. DEPARTMENT OF THE INTERIOR
U.S. GEOLOGICAL SURVEY

COMPILATION OF 20 SONIC AND DENSITY LOGS FROM 12 OIL TEST WELLS ALONG LARSE LINES 1 AND 2, LOS ANGELES REGION, CALIFORNIA

By

Thomas M. Brocher[1], April L. Ruebel[1], Thomas L. Wright[2], and David A. Okaya[3]

Open-File Report 98-366

[1]U.S. Geological Survey, 345 Middlefield Road, M/S 977, Menlo Park, CA 94025
[2]136 Jordan Ave., San Anselmo, CA 94960
[3]Dept. Earth Sciences, University of Southern California, Los Angeles, CA 90089-0740

1998

ABSTRACT

Three-dimensional velocity models for the Los Angeles area provide a means for better understanding the spatial distribution of strong ground motions recorded during earthquakes in southern California. To help constrain such velocity models, deep-crustal wide-angle seismic profiles across the San Fernando Valley and Los Angeles basin were obtained during the Los Angeles Region Seismic Experiment (LARSE).

We have compiled 20 sonic and density logs from 12 oil test wells in the Los Angeles basin and San Fernando Valley to better allow us to determine the geometry and physical properties of these Cenozoic basins along LARSE Lines 1 and 2. The test wells are between 1.2 and 4.3 km deep. Five wells are located in the San Fernando Valley, three wells are located within the San Gabriel Valley, and the remaining four wells are located within the Los Angeles basin between the Whittier and Newport-Inglewood faults. These well logs sample Quaternary to Oligocene sedimentary rocks (principally the Plio-Pleistocene freshwater sands, Saugus, Pico, Repetto, Modelo, Puente, and Topanga Formations), and bottom in variety of sedimentary, volcanic, igneous and metamorphic rocks. This report provides plots showing the density, sonic velocities, and calculated two-way travel times as a function of depth for each well log, and summarizes the linear regression of the data to better understand the velocities and densities of Cenozoic sedimentary rocks in the Los Angeles area.

The three wells from the San Gabriel Valley exhibit a prominent reversal in sonic velocity associated with the contact between non-marine mainly Pleistocene sands and older marine sedimentary rocks at well depths between 1.2 and 1.75 km. Sonic velocities within the overlying non-marine mainly Pleistocene sands and gravels show considerable scatter. In contrast, the underlying marine sedimentary rocks show little scatter in sonic velocity and are as much as 1 km/s slower than the overlying mainly Pleistocene freshwater sands. Evidence for a comparable reversal in sonic velocity at this contact is lacking at the Murphy-Whittier #304 well near the Whittier Fault, and at the Northam Station Corehole #1 well along the Anaheim Nose. A well lying several km northeast of the Newport-Inglewood fault (Hazard #1), exhibits a reversal in sonic velocity in the thin (0.15 km) section of upper Miocene Mohnian stage rocks sampled in the well. A thinner, less prominent sonic low-velocity zone is also observed in the San Fernando Valley.

Surficial compressional-wave velocities inferred by linear projection of regression lines fit to the sonic velocity data fall between 1.8 and 2.4 km/s, with average vertical velocity gradients ranging between 0.59 and 0.79 km/s/km.

These well data suggest that a prominent P- and S-wave low-velocity zone within the Cenozoic basin fill underlies the entire San Gabriel Valley and possibly the margins of the Los Angeles basin. This low-velocity zone should produce large-amplitude guided and converted arrivals at low frequencies (1 to 2 Hz). Thus mapping its extent from other well logs in the Los Angeles basin may allow us to better understand the spatial distribution of strong ground motions in the Los Angeles area.

CONTENTS

TABLE

FIGURES

INTRODUCTION

We present data from 20 sonic and density logs from 12 oil test wells in the San Fernando Valley, San Gabriel Valley, and the Los Angeles basin to help develop a three-dimensional velocity model for the Los Angeles area (Figs. 1 and 2). These 3-D models will be used to calculate synthetic seismograms to improve understanding of strong ground motions in the Los Angeles region [e.g., Magistrale and others, 1996; Hauksson and others, 1997]. The well log data also supplement deep-crustal wide-angle seismic data recorded during the Los Angeles Region Seismic Experiment (LARSE) in October, 1994 [Brocher and others, 1995; Fuis and others, 1996; Murphy and others, 1996; ten Brink and others, 1996].

The locations, elevations, and depths of the oil test wells, as well as the lease name, well number, operator, and completion year are presented in Table 1. In this table, the wells are ordered by latitude from north to south for the wells in San Fernando Valley and similarly for the wells in the San Gabriel Valley and the Los Angeles basin. This information is taken without verification from the Well History Control System (WHCS) One-line File, an on-line digital well-log database leased from Petroleum Information by the USGS Office of Energy Resources at Denver. Table 1 also indicates which of these wells were deviated. Because the logs were run over a 29-year interval between 1962 and 1991, Table 1 provides information on the type of sonic and density tool used to make the log, as well as the other tools run simultaneously (normally caliper, spontaneous potential, and gamma-ray). Several of the sonic logs were made with older tools, with relatively short-spacings between the source and receivers.

BOREHOLE STRATIGRAPHY

Table 2 provides information on the stratigraphy encountered in the boreholes, mainly based on micro and macro biostratigraphy, electric-log correlations, and radiometric dating of ash falls. Age control is available for all of the wells. The following summary of the stratigraphy of the Los Angeles basin is largely derived from Yerkes and others [1965], Blake [1991], and Wright [1991]. Broadly speaking, the middle Miocene to the lower Pleistocene was a time of basin

subsidence and deposition of marine clastic sedimentary rocks followed by a subsequent period of middle Pleistocene to Recent uplift and deposition of non-marine sediments.

As summarized by Yerkes and others [1965], stratigraphic columns in the vicinity of Whittier Narrows show nonmarine sand and gravel, Pleistocene (?) marine sand and silt, the upper Pliocene Pico Formation (a marine sandstone and siltstone, with minor lenses of conglomerate), the lower Pliocene Repetto Formation (a marine coarse-grained sandstone, siltstone, and conglomerate), and the middle-to-upper Miocene Puente Formation (a marine sandstone, siltstone, and shale with minor lenses of conglomerate). In the vicinity of the Long Beach oil field, the upper Pico Formation consists of marine siltstones and sandstones, the middle and lower Pico Formation contains marine sandstones and interbedded siltstones, and the lower Pliocene Repetto Formation consists of petroliferous marine sandstones, minor siltstones, and shales [Yerkes and others, 1965].

In the western Puente Hills area, the Soquel Member of the Puente Formation is a coarse-grained to gritty sandstone with interbedded siltstone. The lower-to-middle Miocene Topanga Formation consists of marine sandstone and siltstone [Yerkes and others, 1965]. The underlying Vaqueros and Sespe Formations, of late Eocene to early Miocene age, consist chiefly of nonmarine clastic sedimentary rocks (sandstones and minor conglomerates) [Yerkes and others, 1965; Blake, 1991].

Blake [1991] has reviewed the stratigraphic nomenclature in the Los Angeles basin and related the local foraminiferal stages to worldwide chronostratigraphic zonation. That zonation shows that most of the lower Mohnian stage, and most of the lower member of the Puente formation, is of middle Miocene age. It also shows that the "Delmontian" stage, considered the uppermost Miocene interval in the Los Angeles basin, actually extends into early Pliocene time. The nodular shale intersected in the Hazard #1 well occurs at the base of the Puente Formation [Blake, 1991].

Middle Miocene rocks of the Luisian stage contain a wide-spread volcanic sequence at their base [Yerkes and others, 1965]. These volcanics are overlain by organic-rich marine clastic rocks and a locally unique schist breccia.

At the Anaheim Nose the middle Miocene Topanga Formation is composed of marine siltstone, sandstone, and conglomerate. The underlying Vaqueros-Sespe Formation undifferentiated, consists of interbedded marine and non-marine clastic sedimentary rocks [Yerkes and others, 1965].

The four wells in San Fernando Valley all sample the Saugus (Sunshine Ranch Member), Pico, Towsley, and Modelo Formations (Table 2). These formations, as exposed in the Santa Susana Mountains, were described by Winterer and Durham [1958]. The Modelo Formation is chiefly siltstone of Luisian and Mohnian stage (middle and late Miocene). The Towsley Formation is composed primarily of sandstones, conglomerates, and mudstones of late Miocene and early Pliocene age. The Pico Formation consists of marine siltstones, sandstones, and conglomerates of Pliocene age. The Sunshine Ranch member of the Saugus Formation interfingering marine, brackish-water, and nonmarine sedimentary rocks. The member consists chiefly of siltstones and sandstones of late Pliocene to early Pleistocene age [Winterer and Durham, 1958; Saul, 1975]. Three of the San Fernando Valley wells sample the Topanga Formation as well. In the Santa Susana Mountains the Topanga Formation consists of sandstones and shales of middle Miocene age [Saul, 1975]. The Leadwell #1 and Hazeltine Core Hole #1 bottomed in quartzdioritic and granitic basement rocks, respectively.

WELL LOG ANALYSIS

Sonic and density logs from the five wells in San Fernando Valley were commercially digitized at 0.5 foot (0.152 m) intervals. For the sonic log from the Burnet #1 well, we corrected the digitized transit times by subtracting 100 μs/ft from them in order to eliminate a large offset in the sonic velocity between the digitized logs from Burnet #1 and #2 at depth of 700 m. Prior to this correction, the sonic velocities calculated from the Burnet #1 sonic log were generally less than

1500 m/s. For the Hazeltine #1 and Leadwell #1 density logs, the quantity digitized is the scintillometer counts/second. There is no ready conversion from counts/sec to g/cm^3 (L. Beyer, pers. comm., 1998). None of the commercially digitized well logs have been edited to remove anomalous values probably associated with washouts, thick mudcake, or invasion of drill fluids.

Sonic and density logs for the remaining wells were hand digitized at non-uniform intervals between 3 and 30 m to capture the significant variations of the logs with depth for frequencies up to 2 Hz. The sampling interval was adequate to estimate linear trends in the data over these intervals. We note that this sampling interval is not sufficiently dense for the calculation of high-frequency (say >10 Hz) synthetic seismograms. For higher-frequency synthetics, it would be necessary to redigitize the logs with a finer sampling interval.

For the sonic logs, we picked transit times as a function of depth down the well. For the gamma-gamma density logs, we picked bulk density in g/cm^3 as a function of depth down the well. For the neutron density porosity logs, we converted the logged density porosity (ϕ) back to formation density (ρ_{fd}) using $\rho_{fd} = \rho_m + (\rho_f - \rho_m)\phi$, where the matrix density $\rho_m = 2.65$ g/cm^3, and the fluid density $\rho_f = 1.0$ g/cm^3 [Ellis, 1987]. All logs presented here were digitized from analog records recorded at a scale of 30.49 m = 5 cm (100 feet = 2 inches). Well depths are measured from an arbitrary reference datum on the drilling platform, usually located about 3.65 m (12 feet) above ground level. The downhole depths reported here have not been corrected to the ground level datum. Cased intervals of the wells and sections identified on the logs as having cycle skipping problems were not digitized. In some cases data from the logs were ignored; these data were associated with washouts, thick mudcake, invasion of drill fluids or large deviations from the general trend of density and sonic values that generally have less than 10 meters depth extent [Ellis, 1987].

The digitized sonic-log data were converted from transit times to velocities (m/s) and both the sonic- and density-logs depths were converted from feet to meters. Figures 3 through 21 show seismic velocities and densities as a function of depth for each well. Although we digitized all

repeated passes of tools in sections of the wells, we do not show these redundant passes in Figures 3 to 21.

Figure 22 presents synthetic seismograms calculated from the well log data from the wells in the San Fernando Valley. Both the sonic and density logs were used to calculate these synthetic seismograms using a convolutional model of the reflection coefficient series with the source wavelet. Neither multiple reflections nor transmission attenuation effects were included in these synthetics. The source wavelet was selected to match that of seismic reflection profiles located near these wells and consisted of a 8 to 36 Hz Ricker wavelet. Note that the amplitudes of the synthetic seismograms for the Leadwell #1 and Hazeltine Core Hole #1 wells are incorrect, since the density logs for these wells are in scintillometer counts/sec.

Figures 23 to 33 present two-way time-depth curves calculated from the interval velocities digitized from the logs. These curves are included to provide guidance for the interpretation of seismic reflection data in the vicinity of the boreholes.

We caution that we have not attempted to independently verify the accuracy of the data that are presented here in digital form. In commercial, open-hole geophysical well logging, there are many sources of possible errors. Such independent data could be bulk density measurements for the density logs and (downhole) seismic check-shot surveys for the sonic logs. Thus, we have not yet determined the absolute or even relative accuracy of these digital data. On the other hand, the general similarities between wells from the same basins, suggests that the general conclusion reached here, that there is a velocity and density reversal with depth (associated with the upper Miocene, fine-grain marine sandstones, siltstones, and shales), is correct.

Finally, we emphasize that plots of the deviated wells indicated in Tables 1 and 2 do not show vertical depth but instead show drilled or inhole depth. Table 2 provides the data necessary to make the correction from drilled or inhole depth to vertical depth.

INTERPRETATION OF WELL LOG DATA

San Gabriel Valley

Logs from all three wells in the San Gabriel Valley display reversals of sonic velocity and density. The most prominent reversal in sonic velocity and density occurs at the Ferris #1 well, beginning at a well depth of 1.75 km, where the compressional wave velocity (Vp) drops almost 1 km/s and density drops nearly 0.2 g/cm^3 (Fig. 5). The section exhibiting low sonic velocity and density is approximately 0.8 km thick. The sonic log from the adjacent Live Oak Park Corehole #1, located 3.5 km northwest of the Ferris #1 well, shows a reversal in sonic velocity at a depth of 1.27 km (Fig. 4). The sonic log from the Consolidated Rocks Product #1 well, 10 km northeast of the Ferris and Live Oak Park Corehole wells, has two reversals, a short one at 1.0 km depth, and a thicker reversal that starts at 1.5 km depth (Fig. 3).

Based on the formations sampled in the boreholes (Table 2), the observed reversal of sonic velocity and density in the San Gabriel Valley occurs at or near the contact between the poorly-sorted freshwater sands and gravels near the base of the Pleistocene and the underlying marine clay-rich sedimentary rocks of early Pleistocene to middle Miocene age [Yerkes and others, 1965; Wright, 1991]. This unconformity is best developed in the northern Los Angeles basin region. The lower scatter of velocity and density measurements in the upper marine section is evidence for the relatively homogenous lithology of this unit, and distinctly constrasts with the higher scatter in sonic velocities and densities measured in the overlying non-marine sedimentary rocks in these wells.

Los Angeles Basin

Logs from two wells in the Los Angeles basin display smaller reversals of sonic velocity and density. There is a small reversal in velocity at the Kellogg #1 well, at a depth of about 1020 m (Fig. 8). Above this level the sonic velocities show more scatter and slightly higher values than those beneath this level. The youngest Miocene rocks in the Hazard #1 well exhibit a minor reversal in sonic velocities (Fig. 9).

The Northam Station Core Hole #1, Kellogg #1, and Hazard #1 wells all sample thick sections of the middle to upper Pliocene Pico and Repetto Formations, and bottom in the Miocene? Topanga or Sespe Formations (Figs. 7 to 9). Sonic velocities measured within the Pico Formation show a well-defined vertical velocity gradient and less scatter than the sonic velocities in the underlying Repetto Formation.

San Fernando Valley

All the sonic logs from the San Fernando Valley exhibit a thin, up to 200 m thick, low velocity zone at a well depth of about 800 m (corresponding to the Saugus, Pico, and Modelo Formations). This low velocity zone lowers the sonic velocity by as much as 0.5 km/s over adjacent portions of the wells. A minor density reversal in the same depth range is also apparent in the density logs for the Hazeltine #1, Leadwell #1, and Burnet #2 logs (Figs. 18, 20-21).

Sonic velocities at the base of both the Hazeltine #1 and Leadwell #1 wells in the San Fernando Valley both raise steeply to values in excess of 4 km/s (Figs. 12 and 13). These wells were documented to have penetrated crystalline basement, so that these relatively high velocities are estimates of the velocities of acoustic bedrock.

Average Velocity Versus Depth Gradients

To estimate average compressional-wave velocity gradients for the Cenozoic sedimentary units in the Los Angeles area, we have performed linear regressions of the sonic velocities for the Plio-Pleistocene freshwater sands, the Pico and Repetto Formations, and Mohnian stage in the San Gabriel Valley and the Los Angeles basin (Tables 3 and 4). For each formation, three columns in Tables 3 and 4 display the resulting projected sonic velocity at the surface, the vertical sonic velocity gradient, the R^2 of the linear fit to the data, and depth interval for which the regression was performed. There is ample evidence in the literature that velocity versus depth relations in Cenozoic sedimentary basins become increasingly non-linear at shallowing depths. The upward

extension of linear regression lines therefore is only a first-approximation of the velocities of the surficial deposits.

DISCUSSION

We next discuss how these estimates of compressional wave velocities within the Cenozoic basins compare to a previous estimate. We then compare the borehole measurements made in the San Gabriel Valley and Los Angeles basin. Finally, we discuss how shear-wave velocities might be related to these sonic velocities.

San Gabriel Valley

The average velocity versus depth relation within the Plio-Pleistocene freshwater sands from the three well logs in Table 3, Vp (km/s) = 2.09 + 0.9Z (Z in km), closely matches that of the k=238 velocity curve selected by Magistrale and others [1996] to depths of 2.5 km. The misfit between this average linear trend inferred from these sonic logs and the k=238 curve used by Magistrale and others [1996] is less than 0.5 km/s except near the surface. The larger misfit at the surface occurs where the k=238 curve is most non-linear and becomes asymptotic to lower velocities (1.2 km/s) than our linear projection of the well log data.

Similarly, linear regression of the sonic log data suggests that, with the exception of the Consolidated Rock Product (CRP) #1 well, velocities inferred from the well log data in the Mohnian stage and older rocks, are on average, only 0.2 to 0.3 km/s lower than the velocities predicted by the k=238 curve selected by Magistrale and others [1996] at depths between 2 and 5 km.

Los Angeles Basin

Sonic velocities within the Pliocene Pico and Repetto Formations in the Los Angeles basin can be better approximated with a single linear velocity-depth curve than can the well logs from the San Gabriel Valley (Figs. 6 to 9; Table 4). Compared to well logs from the San Gabriel Valley,

linear regressions determined for the entire depth extent of the four sonic well logs in the Los Angeles Basin have (1) higher R^2 values (between 0.61 and 0.81), (2) similar projected surface velocities between 1.8 and 2.4 km/s, and (3) lower vertical velocity gradients between 0.59 and 0.70 km/s/km (Table 4). An average velocity curve based on these regressions, Vp (km/s) = 2.01 + 0.64Z (Z in km), lies about half-way between the k=238 and k=200 curves shown by Magistrale and others [1996].

Implications for Shear-Wave Velocity Models

The most obvious and important result from our analysis of the sonic velocity logs is the pronounced low velocity zone at the base of the Plio-Pleistocene freshwater sands, at least within the San Gabriel Valley. Would one also expect these variations with depth to be present in shear wave velocity-depth profiles for these wells? Castagna and others [1985] compiled shear-wave velocity (Vs) and compressional-wave velocity (Vp) data from shear-wave and compressional-wave logging and other measurements to obtain Vp/Vs for a variety of clastic silicate rocks. Castagna and others [1985] suggest that Vp/Vs ratios in sandstones reach an average value near 1.7 beginning at depths of about 2 km, whereas the Vp/Vs in noncalcareous shales reach an average value of about 2 at depths near 3 km. Thus, from the published compilations of Vp/Vs ratios in Tertiary sedimentary rocks we would expect that the presence of a 20 to 25% reversal of sonic velocity and an 8 to 10% reversal in density at the Plio-Pleistocene freshwater/marine boundary in the San Gabriel Valley will be accompanied by a similar reversal in shear-wave velocity [Ohta and others, 1997; Hamilton, 1979; and Castagna and others, 1985]. Strong shear wave conversions, reflections, and guided waves are expected at this boundary, at least within the San Gabriel Valley. Existing three-dimensional velocity models for the Los Angeles basin do not incorporate a velocity reversal within the Cenozoic basin fill (e.g. Magistrale and others [1996] and Hauksson and others [1997]).

DATA AVAILABILITY

The picks of density, sonic velocity, and two-way travel times versus depth shown in Figures 3 to 21 and 23 to 33 are available in Excel5 spreadsheets using anonymous ftp. The anonymous ftp address is: andreas.wr.usgs.gov. Change the directory (cd) to /pub/outgoing/larse. The Excel5 files are named larse.sonic.xl5.bin, larse.tt.xl5.bin, and larse.density.xl5.bin, in Mac Binary II format. Due to the large size of the files for each of the digitized well logs from the San Fernando Valley, individual files for each of the sonic and density logging runs are provided. Table 1 of this report in Excel5 format is also in this ftp site, labeled as Table 1.bin. The text is in a Word 5 formatted file named OFR.text.bin. Figures 1 and 2 are in Adobe Illustrator 6 format in files OFR.Fig1 and OFR.Fig2.

SUMMARY

We compiled 20 sonic and density logs from 12 oil test wells in the Los Angeles region to better allow us to determine the geometry and physical properties of these Cenozoic basins in the Los Angeles area. The test wells are between 1.2 and 4.3 km deep. Five of the wells are located in the San Fernando Valley, three wells are located within the San Gabriel Valley, and the remaining four wells are located within the Los Angeles basin between the Whittier and Newport-Inglewood faults.

These well data suggest that a prominent P- and S-wave low-velocity zone within the Cenozoic basin fill underlies the entire San Gabriel Valley and possibly the northern margins of the Los Angeles basin. The three wells from the San Gabriel Valley exhibit a prominent reversal in sonic velocity associated with the contact between non-marine mainly Pleistocene sands and older marine sedimentary rocks. This low-velocity zone should produce large-amplitude guided and converted arrivals at low frequencies (1 to 2 Hz). Thus mapping its extent from other well logs in the region may allow us to better understand the spatial distribution of strong ground motions in the Los Angeles area.

ACKNOWLEDGEMENTS

Zenon Valin, USGS, kindly performed a search of a digital database providing well locations and other well information. Vicki Langenheim, USGS, drafted Figures 1 and 2. John Tinsley, USGS, guided us to references on the stratigraphy in the San Fernando Valley. Gary Fuis and Larry Beyer, both USGS, provided helpful comments on an earlier draft of this manuscript.

This work was supported by the National Earthquake Hazards Reduction Program and the Southern California Earthquake Center (SCEC).

REFERENCES CITED

Blake, G.H., 1991, Review of the Neogene biostratigraphy and stratigraphy of the Los Angeles basin and implications for basin evolution, in K.T. Biddle, ed., Active margin basins: AAPG Memoir 52, p. 135-184.

Brocher, T.M., R.W. Clayton, K.D. Klitgord, R.G. Bohannon, R. Sliter, J.K. McRaney, J.V. Gardner, and J.B. Keene, 1995, Multichannel seismic-reflection profiling on the R/V Maurice Ewing during the Los Angeles Region Seismic Experiment (LARSE), California, U.S. Geological Survey Open-File Report 95-228, 73 pp.

Castagna, J.P., Batzle, M.L., and Eastwood, R.L., 1985, Relationships between compressional-wave and shear-wave velocities in clastic silicate rocks, Geophysics, v. 50, p. 571-581.

Crouch, J.S., and J. Suppe, 1993, Late Cenozoic tectonic evolution of the Los Angeles basin and inner California borderland: A model for core complex-like crustal extension, Geological Society of America, Bulletin, v. 105, p. 1415-1434.

Davis, T.L. and J.S. Namson, 1994, A balanced cross-section of the 1994 Northridge earthquake, southern California, Nature, v. 372, p. 167-169.

Ellis, D.V., 1987, Well Logging for Earth Scientists, Elsevier, New York, 532 p.

Fuis, G.S., D.A. Okaya, R.W. Clayton, W.J. Lutter, T. Ryberg, T.M. Brocher, T. Henyey, M. Benthien, P.M. Davis, J. Mori, R.D. Catchings, U.S. ten Brink, M.D. Kohler, K.D. Klitgord, and R.G. Bohannon, 1996, Images of crust beneath Southern California will aid study of earthquakes and their effects, EOS, Trans. AGU, v. 77, p. 173, 176.

Hamilton, E.L., 1979, Vp/Vs and Poisson's ratios in marine sediments and rocks, Journal of the Acoustical Society of America, v. 66, p. 1093-1101.

Hauksson, E., and Haase, J.S., 1997, Three-dimensional Vp and Vp/Vs velocity models of the Los Angeles basin and central Transverse Ranges, California, J. Geophys. Res., v. 102, p. 5423-5453.

Magistrale, H., McLaughlin, K., and Day, S., 1996, Geology-based 3-D velocity model of the Los Angeles basin sediments, Bull. Seism. Soc. Am., v. 86, p. 1161-1166.

Murphy, J.M., Fuis, G.S., Rybert, T., Okaya, D.A., Criley, E.E., Benthien, M.L., Alvarez, M., Asudeh, I., Kohler, W.M., Glassmoyer, G.N., Robertson, M.C., and Bhowmik, J., 1996, Report for explosion data acquired in the 1994 Los Angeles region seismic experiment (LARSE), Los Angeles, California, U.S. Geological Survey Open-File Report 96-536, 120 pp.

Ohta, Y., N. Goto, K. Shiono, H. Takahashi, F. Yamamizu, and S. Kurihara, 1977, Shear wave velocities in deep soil deposits; measurement in a borehole to the depth of 3500 meters and its significance, Jishin Gakkai (Seismological Society of Japan), v. 30, p. 415-433.

Real, C.R., 1977, Seismicity and tectonics of the Santa Monica-Hollywood-Raymond Hill fault zone and northern Los Angeles basin, Los Angeles County, California, Transverse Ranges, U.S. Geological Survey Prof. Paper 1339, p. 113-124.

Saul, R.B., 1975, Geology of the southeast slope of the Santa Susana Mountains and geologic effects of the San Fernando earthquake, in Oakeshott, G.B., ed., San Fernando, California, earthquake of 9 February 1971, Calif. Div. of Mines and Geology, Bulletin 196, p. 53-70.

Shaw, J.H., S.C. Hook, and J. Suppe, 1994, Structural trend analysis by axial surface mapping, AAPG Bulletin, v. 78, p. 700-721.

Shaw, J.H., and J. Suppe, 1994, Active faulting and growth folding in the eastern Santa Barbara Channel, California, Geol. Society of America, Bulletin, v. 106, p. 607-626.

U.S. ten Brink, R.M. Drury, G.K. Miller, T. Brocher, and D. Okaya, 1996, Los Angeles Region Seismic Experiment (LARSE), California off-shore Seismic Refraction data, USGS Open-File Report 96-27.

Winterer, E.L., and D.L. Durham, 1958, Geologic map of a part of the Ventura Basin Los Angeles County, California, U.S. Geological Survey, Oil and Gas Investigations Map OM 196, scale 1:24,000.

Wright, T., 1991, Structural geology and tectonic evolution of the Los Angeles basin, California, in K.T. Biddle, ed., Active margin basins: AAPG Memoir 52, p. 35-134.

Yerkes, R.F., T.H. McCulloh, J.E. Schoellhamer, and J.G. Vedder, 1965, Geology of the Los Angeles basin California--an Introduction, U.S. Geological Survey, Prof. Paper 420-A, 57 pp., 4 plates.

ABBREVIATIONS USED IN TABLE 1:

BHC - Borehole Compensated Sonic Log
CNFD - Compensated Neutron Formation Density*
CFD gg - Compensated Formation Density (gamma-gamma)*
CNF (ds) - Compensated Neutron Formation Density (Dual Spaced)*
Cal. - Caliper
D.F. - Drilling floor
G.L. - Ground level
K.B. - Kelly Bushing
SP - Spontaneous Potential
GR - Gamma Ray

T3R3R - Sonic tool spacing (in feet) between transmitter (T) and receivers (R)

*All density logging tools employ the backscattered gamma-ray technique, commonly called "gamma-gamma". The different names used here are either from different vendors or from different generations (having different trademark names).

Table 1. Oil test well data

Leasename	No.	Operator	ID	Latitude	Longitude	Depth (ft)	Depth (m)	Vertical or Deviated?	T	T	R	R	S	Field	Elev. Datum	Elev. (ft)	Elev. (m)	Completion year	Sonic tool	Density tool	Other tools
Consol. Rock Products	1	Standard Oil Co. of Calif.	5962	34.12726	-117.93741	7479	2280	Vertical	1	N	10	W	33	Azusa	D.F.			1962	T3R3R	Scintillometer	SP
Live Oak Park Corehole	1	Standard Oil Co. of Calif.	21092	34.10205	-118.04545	8695	2651	Deviated	15	S	11	W	9	Temple City	G.L.	353.9	108	1971	BHC T3R2R		Cal., SP
Ferris	1	Standard Oil Co. of Calif.	5964	34.07421	-118.02845	12182	3714	Vertical	1	S	11	W	21	El Monte	G.L.	290	88	1964	BHC T3R2R	CFD gg	Cal., GR, SP
Murphy Whittier	304	Chevron USA Inc.	23652	33.97355	-117.99847	14213	4333	-Vertical	2	S	11	W	26	Whittier	G.L.	818	249	1991	BHC	CNLD	Cal., GR
Northam Station Core	1	Standard Oil Co. of Amer.	20435	33.88087	-118.01779	11500	3506	Deviated	3	S	11	W	27	La Mirada	G.L.	63	19	1968	BHC T3R2R	CFD gg	Cal.
Kellogg	1	Standard Oil Co. of Calif.	1165	33.81581	-117.95458	10229	3119	Deviated	4	S	10	W	20	Anaheim	D.F.	112	34	1962	T3R3R		SP
Hazard	1	Standard Oil Co. of Calif.	20119	33.74134	-117.98273	10730	3271	Deviated	5	S	11	W	13	Midway City	G.L.	35	11	1968	BHC T3R2R		Cal., SP
Burnet Core Hole	1	Chevron USA Inc.		34.2558	-118.4538	10227	3118	Deviated	16	N	2	W	15	Pacoima	G.L.	914	279	1977			
Burnet Core Hole	2	Chevron USA Inc.		34.2558	-118.4538	8981	2738	Deviated	16	N	2	W	15	Pacoima	G.L.	917	280	1978			
Frieda J Clark	1	Chevron USA Inc.	21018	34.22295	-118.51007	7323	2233	Deviated	25	N	2	W	16	San Fernando	G.L.	795	242	1970			
Leadwell	1	Chevron USA Inc.	05974	34.20401	-118.44614	5066	1545	Deviated	3	N	1	W	15	Van Nuys	G.L.	754	230	1963		Scintillometer	
Hazeltine Core Hole	1	Chevron USA Inc.	05969	34.17578	-118.42516	3823	1166	Vertical	14	N	1	W	15	Van Nuys	G.L.	679	207	1963		Scintillometer	

Table 2. Stratigraphy in oil test wells from Los Angeles Basin*.

Well Name	Depth (feet)	Depth (m)	Depth (ft)	Depth (m)
Cons. Rock Prod. No. 1				
	Original hole	Original hole	Redrill	Redrill
Non-marine				
Top/Marine	3110	948.2	2950	899.4
Within U. Mohnian	3300	1006.1	3280	1000.0
1st Mid Mohnian	3550	1082.3	3500	1067.1
Soquel/La Vida	5100	1554.9	5280	1609.8
Within L. Mohnian	5200	1585.4		
est. Top/Luisian	5540	1689.0	5480	1670.7
Top/Non-marines	7020	2140.2		
Top/Volcanics	7060	2152.4		
Live Oak Park CH No. 1				
	Deviated	Deviated	Vertical	Vertical
Base of freshwater sands	4089	1246.6	3809	1161.3
Top/marine Pleistocene	4180	1274.4	3889	1185.7
Top/marine Pliocene	4480	1365.9	4153	1266.2
Top/Mohnian	4700	1432.9	4309	1313.7
Top/Mid. Mohnian	4860	1481.7	4424	1348.8
Top/L. Mohnian	6000	1829.3	5387	1642.4
Top/Luisian	6280	1914.6	5619	1713.1
Top bsmt gneiss	8560	2609.8	7515	2291.2
Ferris No. 1				
1st Marine	5970	1820.1		
Top Mohnian	6385	1946.6		
Top Middle Mohnian	7510	2289.6		
1st Lower Mohnian	10715	3266.8		
Top Luisian	11400	3475.6		
Top granitoid bsmt	12073	3680.8		
Murphy-Whittier No. 304				
	Deviated	Deviated	Vertical	Vertical
in Middle Repetto	888	270.7		
Top/Lower Repetto	2220	676.8	2020	615.9
Top/Miocene	3120	951.2	3119	950.9
Top/Mohnian	4020	1225.6	4013	1223.5
Fault	5580	1701.2	5536	1687.8
undiff. Mohnian	6000	1829.3	5947	1813.1
Fault	8840	2695.1	8773	2674.7
Lower Mohnian	11520	3512.2	11382	3470.1
Topango	12557	3828.4	12410	3783.5
Fault	13030	3972.6	12869	3923.5
Sespe	14092	4296.3	13885	4233.2
Northam Station No. 1				
1st Marine Pleist.	880	268.3		

1st U. Pico	2440	743.9
1st M. Pico	3280	1000.0
1st L. Pico	6840	2085.4
Top Repetto	7760	2365.9
Top Mid Repetto	9490	2893.3
Top Lower Repetto	11015	3358.2
Top Topanga	11180	3408.5

Kellogg No. 1

	Original hole	Original hole	Redrill	Redrill
Top/Pico	3338	1017.7		
Top/Pico	3410	1039.6		
within M. Pico/approx.			7500	2286.6
Top Repetto			8750	2667.7
within Repetto	8200	2500.0		
Top Miocene, highest non-marine	9450	2881.1	10325	
Vaqueros on mega/			11025	3361.3
probable Sespe			11244	3428.0
prob. mid-Miocene	9700	2957.3		

Hazard No. 1

	Vertical	Vertical
1st Marine Pleist.	265	80.8
1st U. Pico	1520	463.4
1st M. Pico	2640	804.9
1st L. Pico	5960	1817.1
Top Repetto	6560	2000.0
Top Mid Repetto	7630	2326.2
Top Lower Repetto	8550	2606.7
Top Miocene	9040	2756.1
Top Mohnian	9240	2817.1
Top Nodular shale	9290	2832.3
Base Nod. Shale/Top Topanga	9768	2978.0

Burnett Core Hole #1

	Deviated	Deviated
Top Sunshine Ranch	1090	332.3
Top Pico (Fernando)	3150	960.4
Top Towsley (U. Mohn.)	4570	1393.3
Top Modelo	5920	1804.9
Top Topanga	9090	2771.3

Burnett Core Hole #2

	Deviated	Deviated
Top Sunshine Ranch	1090	332.3
Top Pico (Fernando)	3330	1015.2
Top Towsley (U. Mohn.)	4880	1487.8
Top Modelo	6330	1929.9

Frieda J. Clark C.H. #1

	Deviated	Deviated
Top Sunshine Ranch	1310	399.4

Top Pico (Fernando)	2650	807.9
Top Towsley (U. Mohn.)	3650	1112.8
Top Modelo	4650	1417.7
Middle Mohnian	6955	2120.4
Top Topanga	7080	2158.5
Top Hollycrest Conglom.	7200	2195.1

Leadwell #1

	Deviated	Deviated
Top Sunshine Ranch	1010	307.9
Top Pico (Fernando)	2460	750.0
Top Towsley (U. Mohn.)	3980	1213.4
Top Modelo	4460	1359.8
Top of quartzdiorite bsmt.	4840	1475.6

Hazeltine Core Hole #1

	Vertical	Vertical
Top Sunshine Ranch	700	213.4
Top Pico (Fernando)	970	295.7
Top Towsley (U. Mohn.)	1990	606.7
Top Modelo	2360	719.5
Top Topanga	3270	997.0
Top of granitic basement	3780	1152.4

*Formation picks are from a combination of micro- and macropaleontology, correlations of electric logs, and radiometric dating of ash fall deposits.

Table 3. Regression of sonic velocities in oil test wells from the San Gabriel Valley.

Well	Regression V_P in freshwater sands (km/s)**	R^2	Depth Interval (km)	Regression V_P below freshwater sands (km/s)**	R^2	Depth Interval (km)
Cons. Rock Prod. #1	2.43 + 0.57 Z	0.156	0 - 0.900	–	–	–
Live Oak Park Corehole #1	1.84 + 1.15 Z	0.628	0 - 1.268	1.29 + 0.83 Z	0.507	1.27-2.65
Ferris #1	2.00 + 0.99 Z	0.465	0 - 1.750	1.69 + 0.74 Z	0.377	1.75-3.71

** Z = depth in well in km.

Table 4. Regression of sonic velocities in oil test wells from Los Angeles Basin.

Well	Regression V_P in Pico and Repetto Fms. (km/s)**	R^2	Depth Interval (km)
Murphy Whittier #304	2.40 + 0.63 Z	0.731	Entire Log
"	2.35 + 0.64 Z	0.431	0 - 1.850
Northam Station Corehole #1	1.97 + 0.63 Z	0.671	Entire Log
Kellogg #1	1.83 + 0.70 Z	0.805	Entire Log
"	1.86 + 0.65 Z	0.716	0 - 2.191
Hazard #1	1.85 + 0.59 Z	0.614	Entire Log

** Z = depth in well in km.

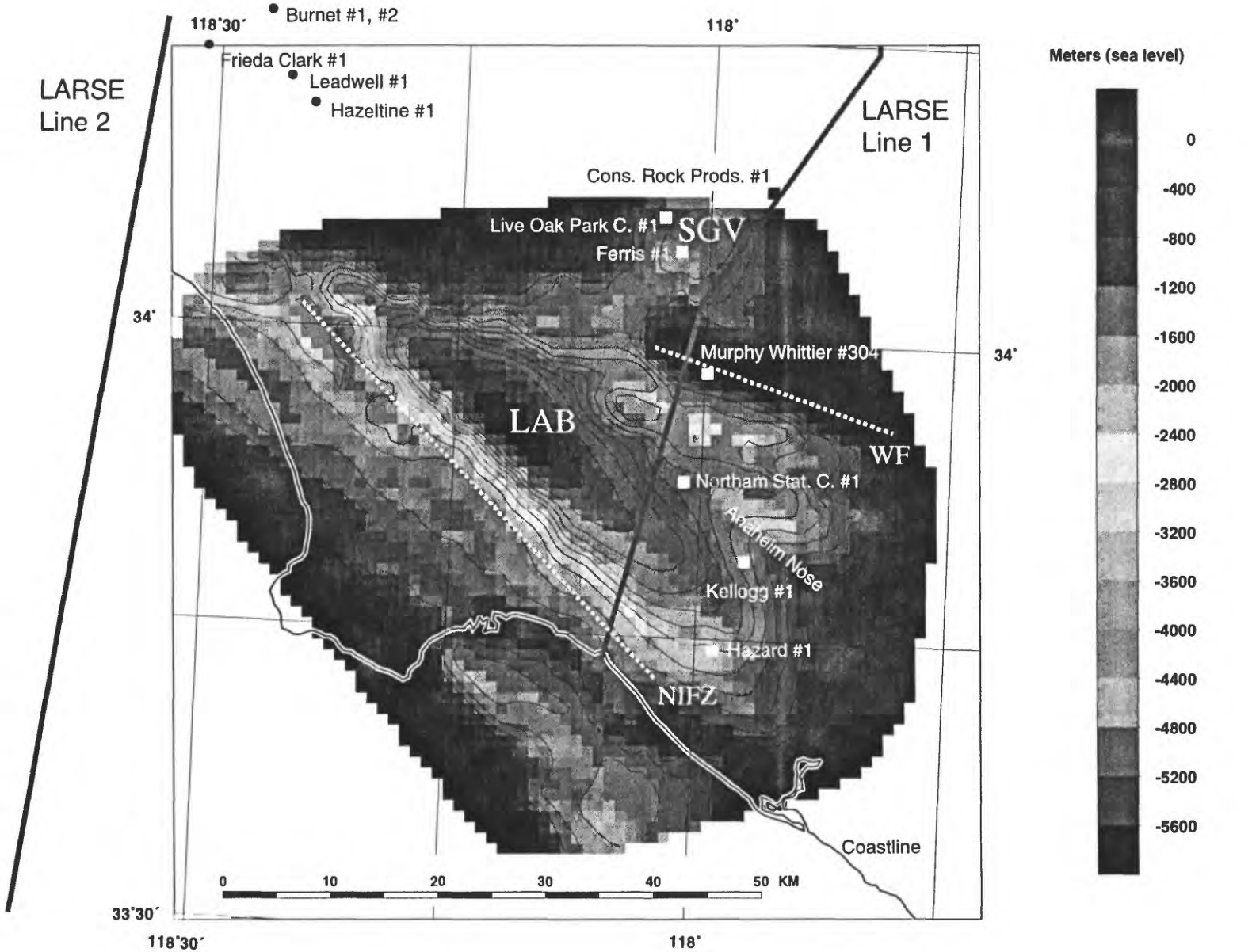

Figure 1. Map of the Los Angeles area showing the base of the Repetto Formation (circa 4.5 Ma) relative to sea level [Wright, 1991], locations of the sonic well logs analyzed here (squares and circles), LARSE Lines 1 and 2, the Los Angeles basin (LAB), the San Gabriel valley (SGV), the Newport-Inglewood fault zone (NIFZ), the Whittier fault (WF), and the coastline.

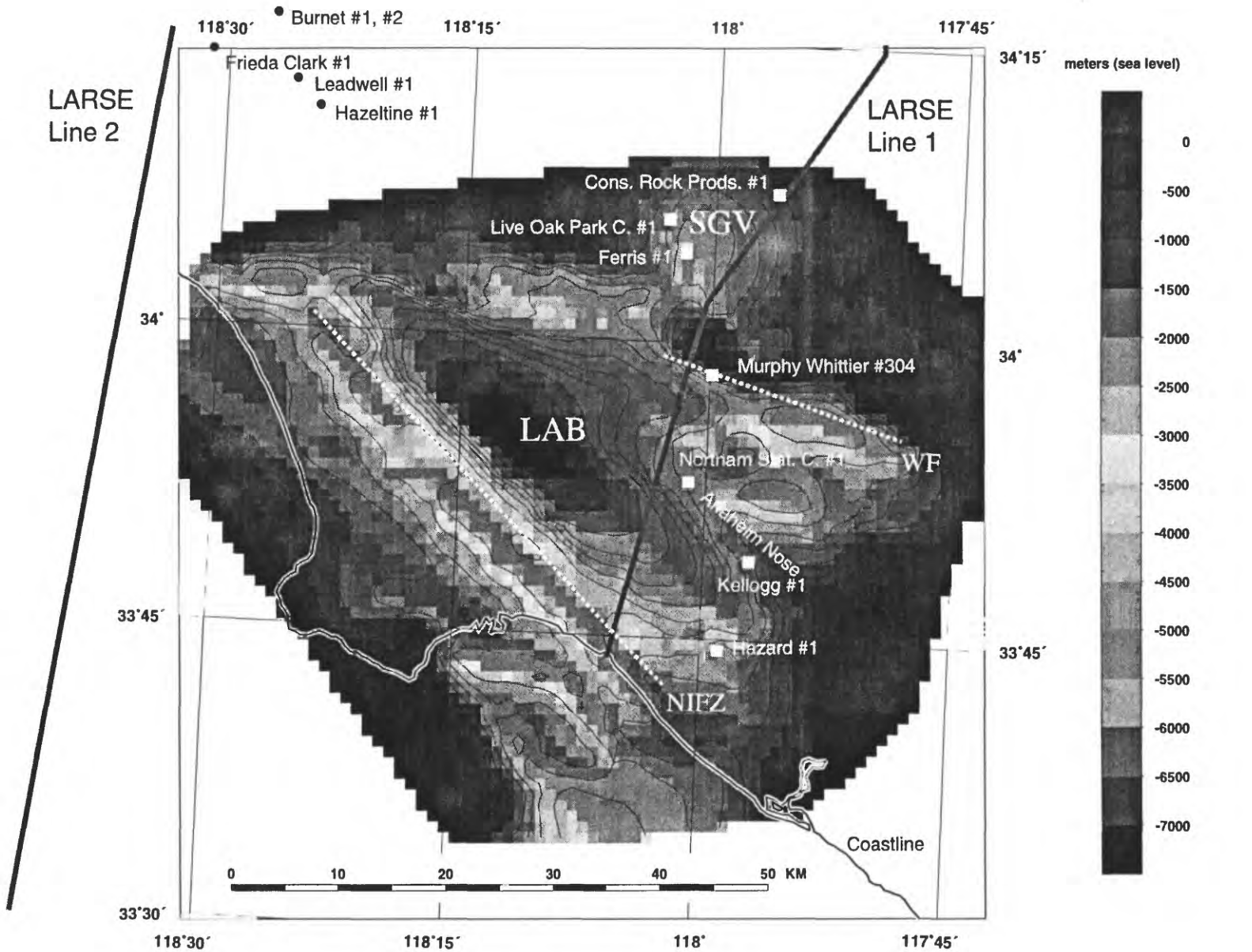

Figure 2. Map of the Los Angeles area showing the base of the Mohnian Stage (circa 14 Ma) relative to sea level [Wright, 1991], locations of the sonic well logs analyzed here (squares and circles), LARSE Lines 1 and 2, the Los Angeles basin (LAB), the San Gabriel valley (SGV), the Newport-Inglewood fault zone (NIFZ), the Whittier fault (WF), and the coastline.

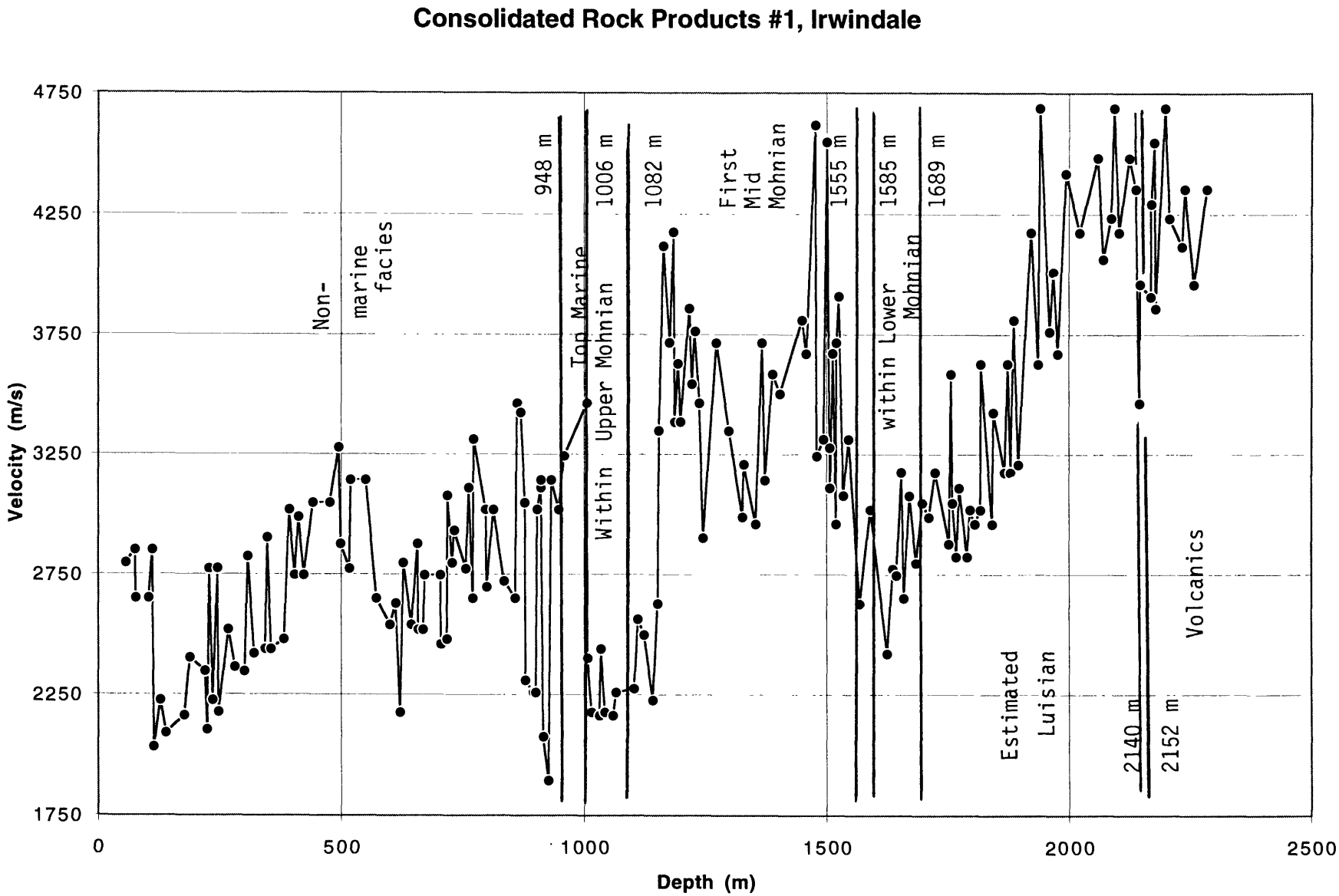
Consolidated Rock Products #1, Irwindale
Velocity (m/s)
4750
4250
3750
3250
2750
2250
1750
0
500
1000
1500
2000
2500
Depth (m)
Non-
marine
facies
948 m
Top Marine
Within Upper Mohnian
1006 m
1082 m
First
Mid
Mohnian
1555 m
1585 m
within Lower
Mohnian
1689 m
Estimated
Luisian
2140 m
2152 m
Volcanics

Figure 3.

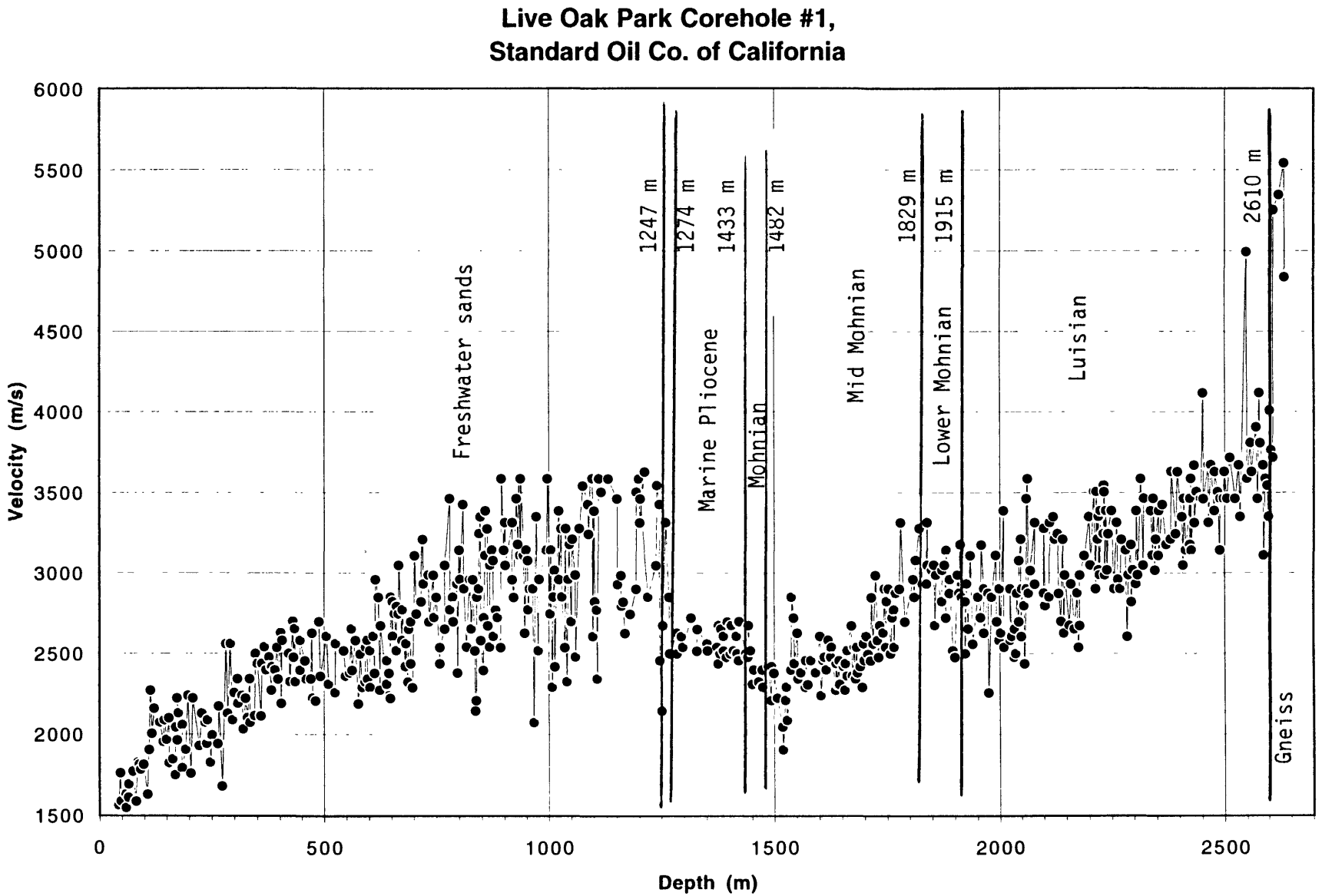
Live Oak Park Corehole #1,
Standard Oil Co. of California
Velocity (m/s)
6000
5500
5000
4500
4000
3500
3000
2500
2000
1500
0
500
1000
1500
2000
2500
Depth (m)
Freshwater sands
1247 m
1274 m
Marine Pliocene
1433 m
Mohnian
1482 m
Mid Mohnian
1829 m
1915 m
Lower Mohnian
Luisian
2610 m
Gneiss

Figure 4.

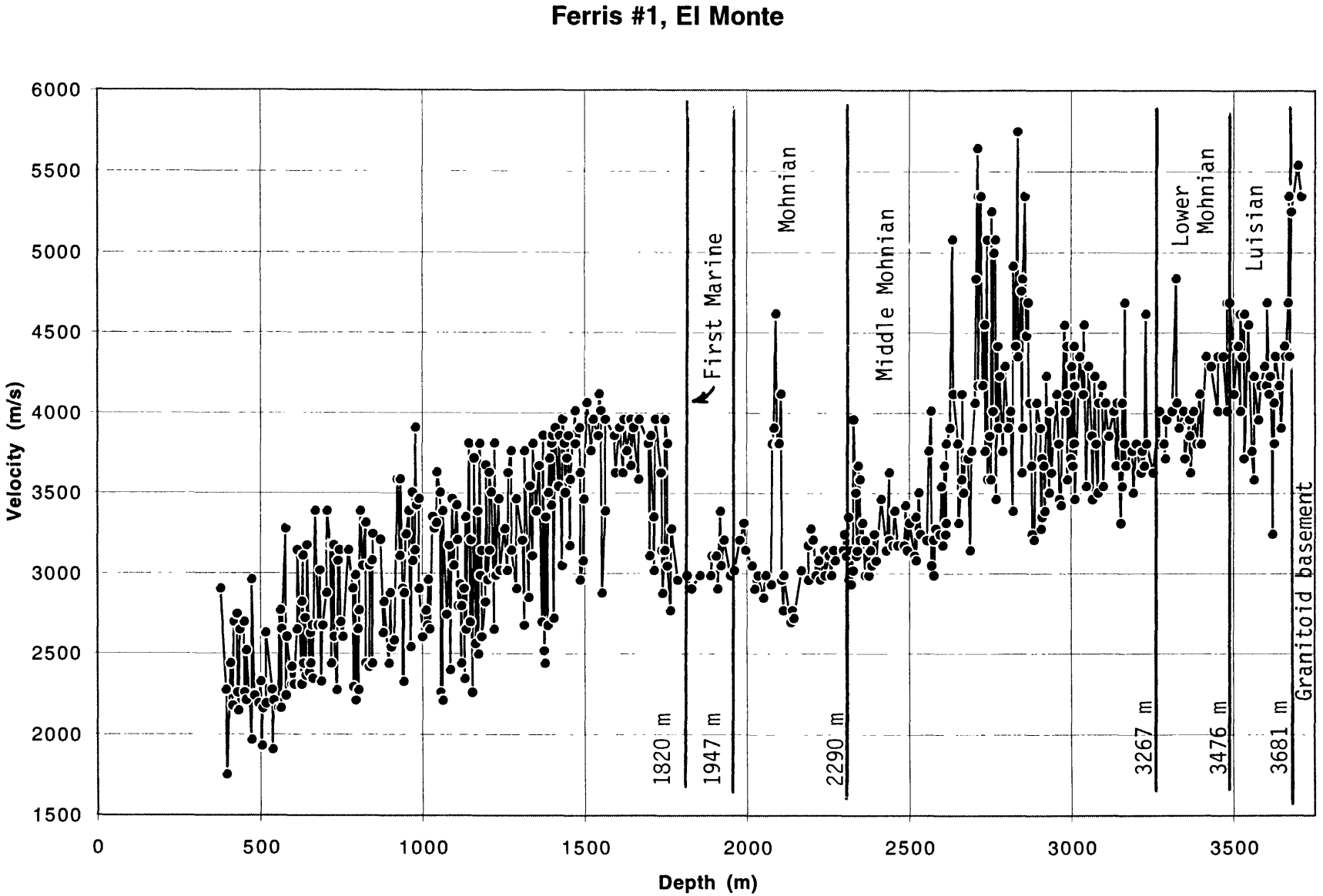
Ferris #1, El Monte
Velocity (m/s)
Depth (m)
6000
5500
5000
4500
4000
3500
3000
2500
2000
1500
0
500
1000
1500
2000
2500
3000
3500
First Marine
Mohnian
Middle Mohnian
Lower Mohnian
Luisian
Granitoid basement
1820 m
1947 m
2290 m
3267 m
3476 m
3681 m

Figure 5.

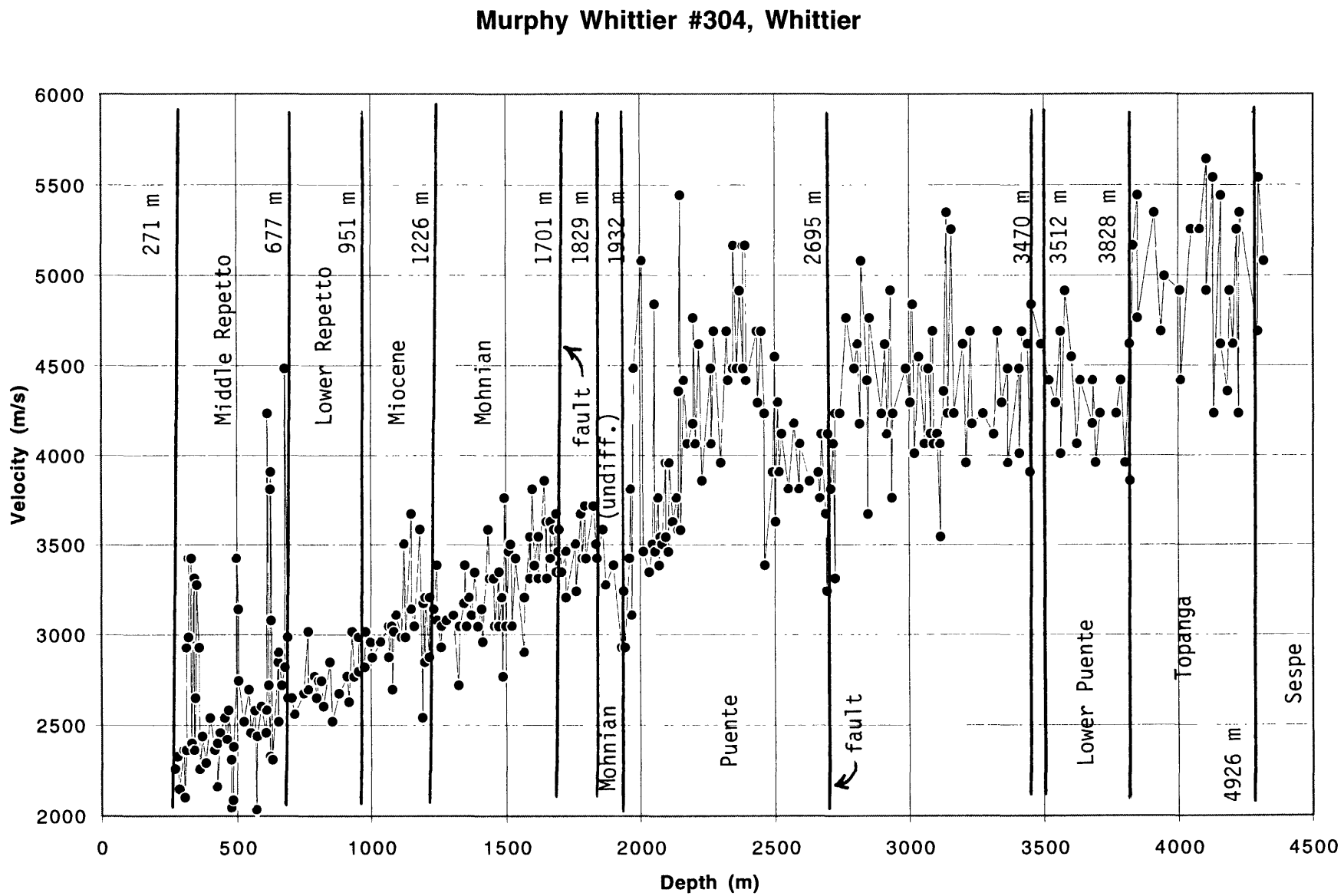
Murphy Whittier #304, Whittier
Velocity (m/s)
Depth (m)
271 m
Middle Repetto
677 m
Lower Repetto
951 m
Miocene
1226 m
Mohnian
1701 m
fault
1829 m
1932 m
(undiff.)
Mohnian
Puente
2695 m
fault
3470 m
3512 m
Lower Puente
3828 m
Topanga
4926 m
Sespe

Figure 6.

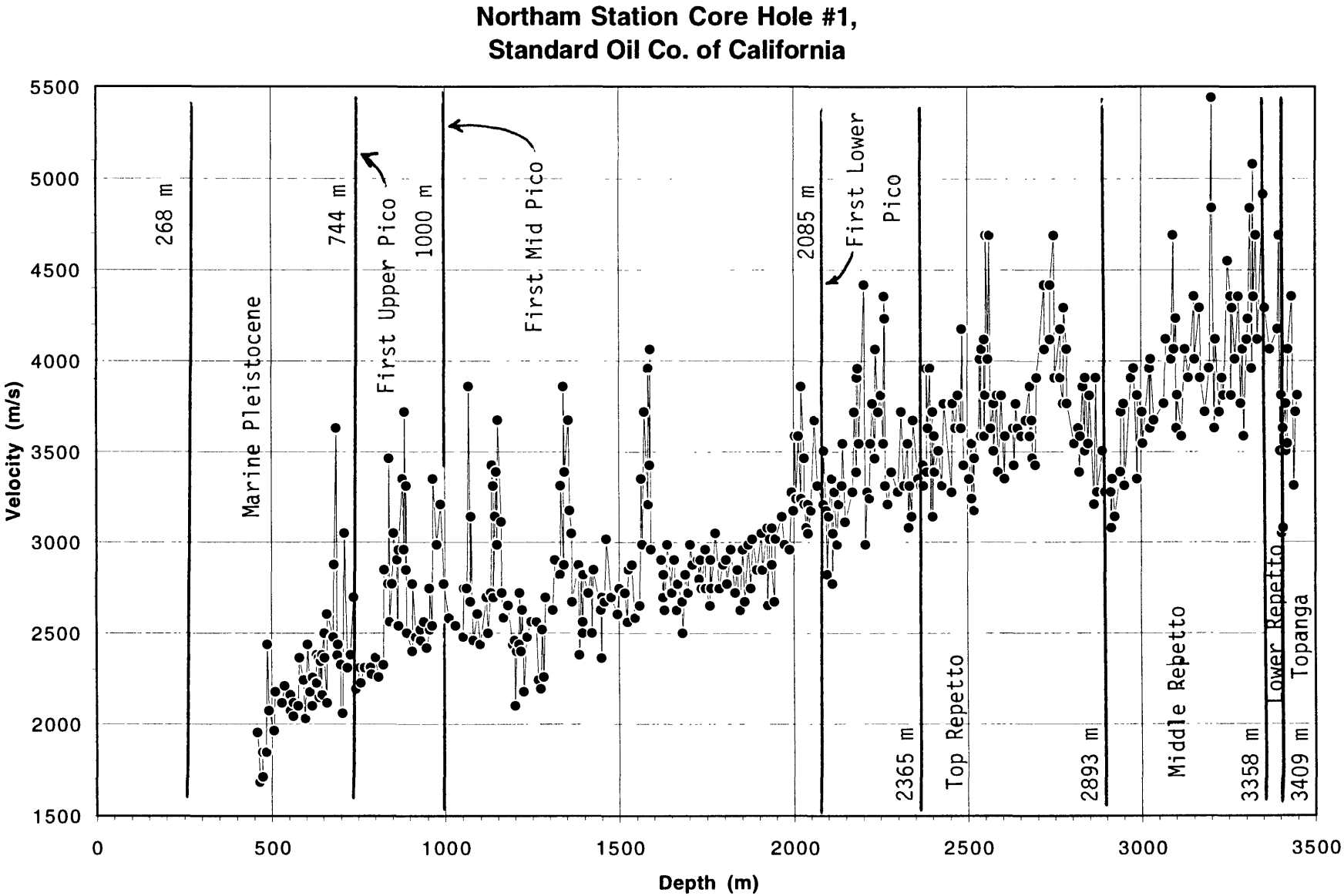
Northam Station Core Hole #1,
Standard Oil Co. of California
Velocity (m/s)
Depth (m)
5500
5000
4500
4000
3500
3000
2500
2000
1500
0
500
1000
1500
2000
2500
3000
3500
268 m
Marine Pleistocene
744 m
First Upper Pico
1000 m
First Mid Pico
2085 m
First Lower Pico
2365 m
Top Repetto
2893 m
Middle Repetto
3358 m
Lower Repetto
3409 m
Topanga

Figure 7.

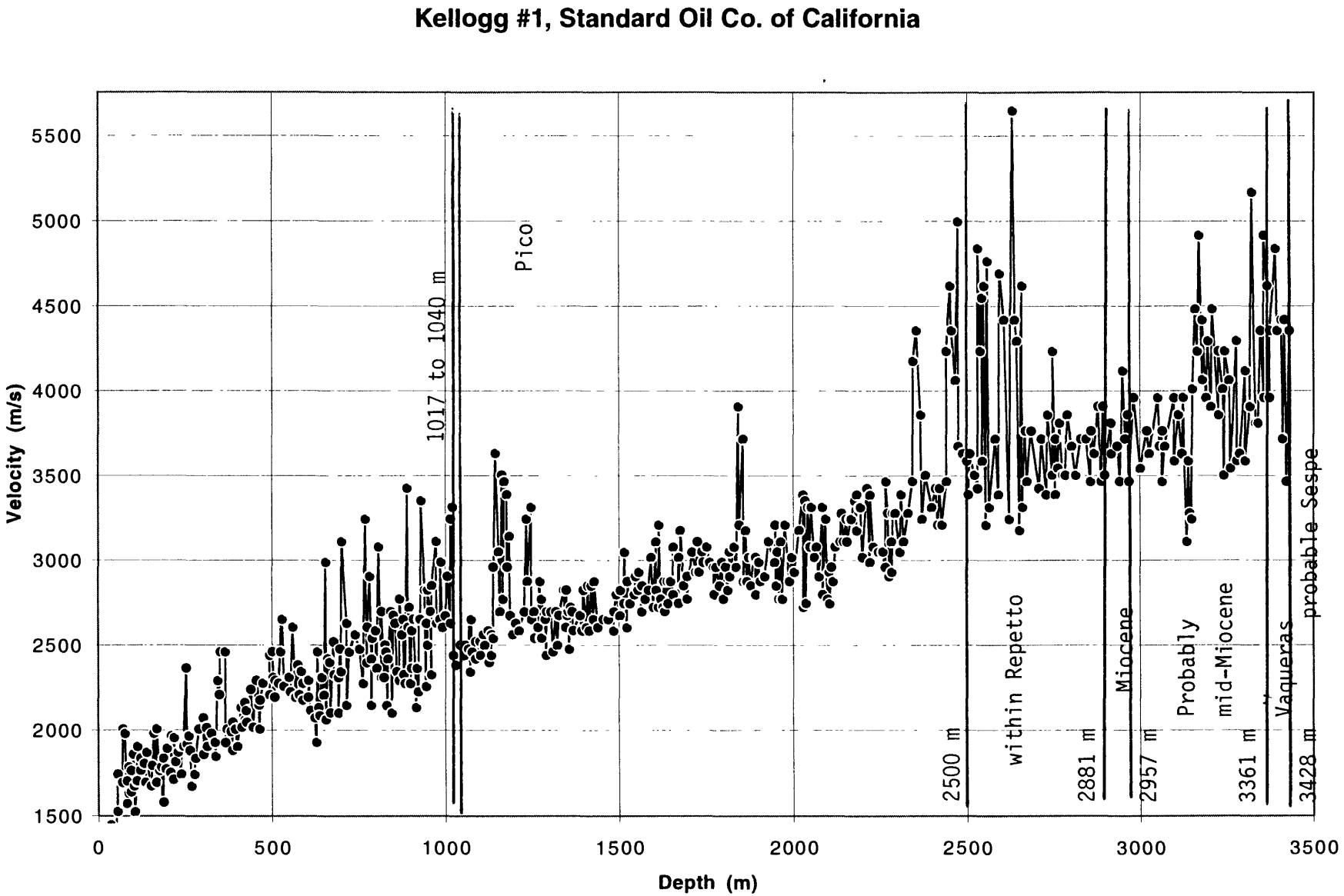
Kellogg #1, Standard Oil Co. of California
Velocity (m/s)
Depth (m)
1017 to 1040 m
Pico
2500 m
within Repetto
2881 m
Miocene
2957 m
Probably
mid-Miocene
3361 m
Vaqueras
3428 m
probable Sespe

Figure 8.

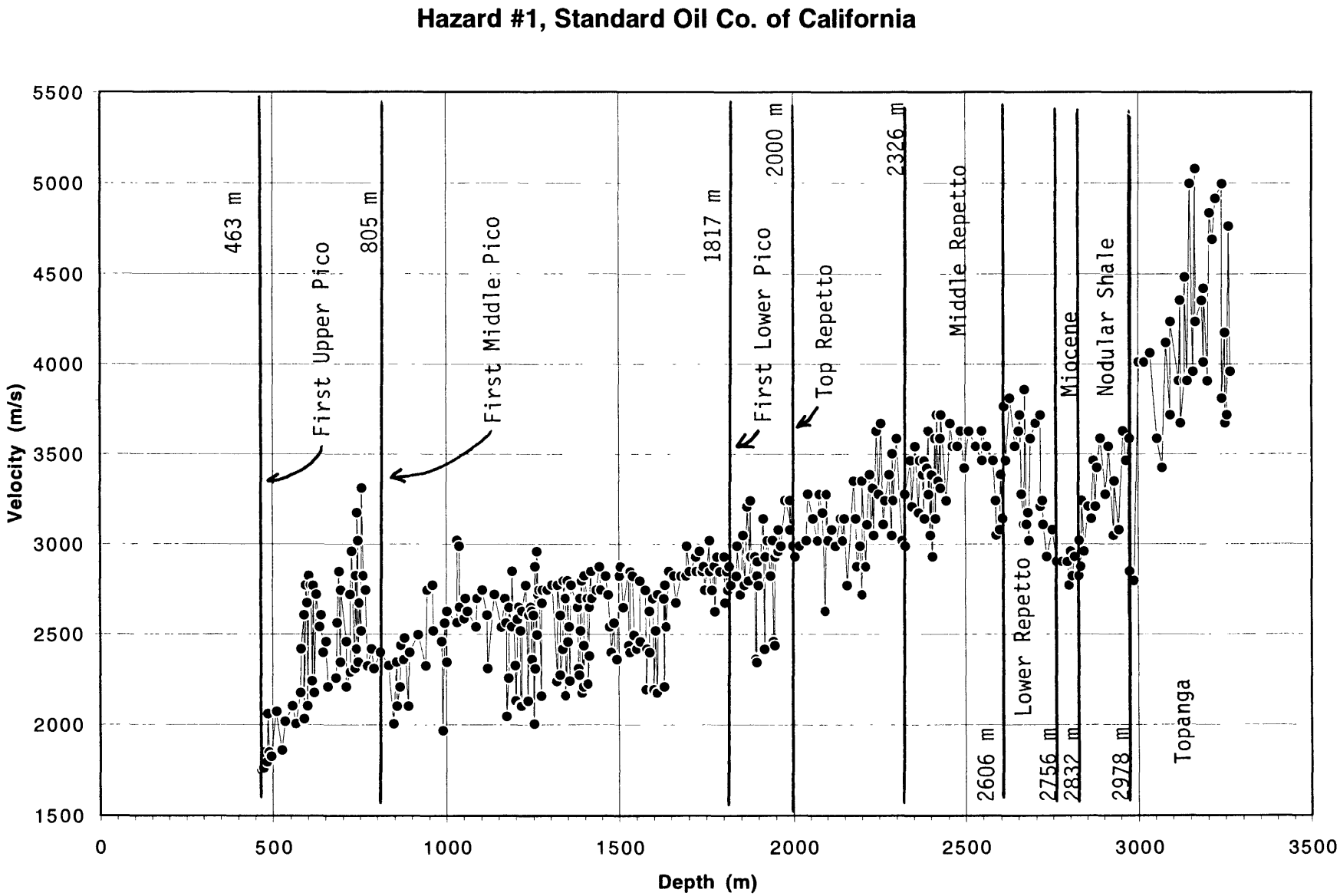
Hazard #1, Standard Oil Co. of California
Velocity (m/s)
Depth (m)
5500
5000
4500
4000
3500
3000
2500
2000
1500
0
500
1000
1500
2000
2500
3000
3500
463 m
First Upper Pico
805 m
First Middle Pico
1817 m
First Lower Pico
2000 m
Top Repetto
2326 m
Middle Repetto
2606 m
Lower Repetto
2756 m
Miocene
2832 m
Nodular Shale
2978 m
Topanga

Figure 9.

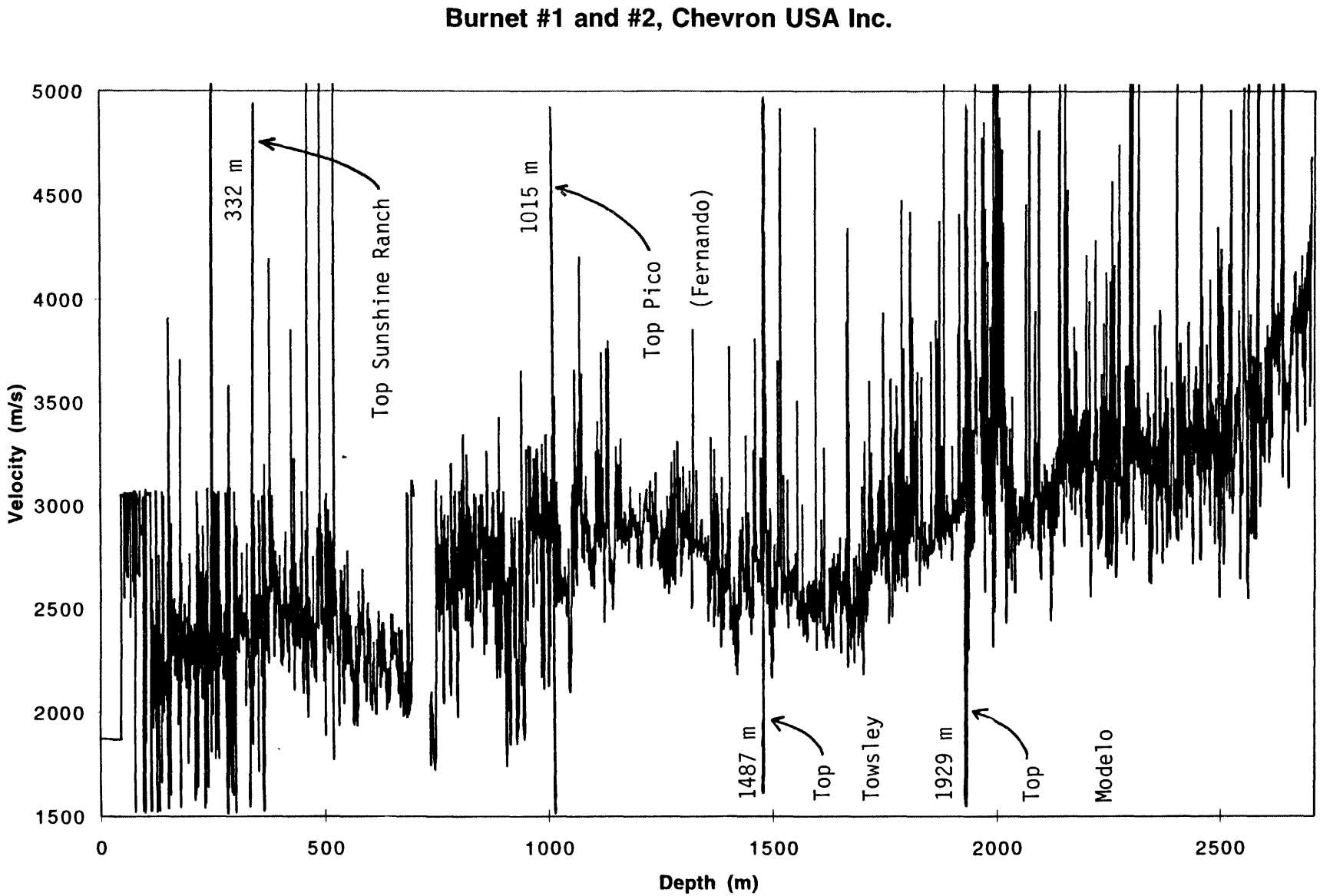
Burnet #1 and #2, Chevron USA Inc.
Velocity (m/s)
5000
4500
4000
3500
3000
2500
2000
1500
0
500
1000
1500
2000
2500
Depth (m)
332 m
Top Sunshine Ranch
1015 m
Top Pico
(Fernando)
1487 m
Top
Towsley
1929 m
Top
Modelo

Figure 10.

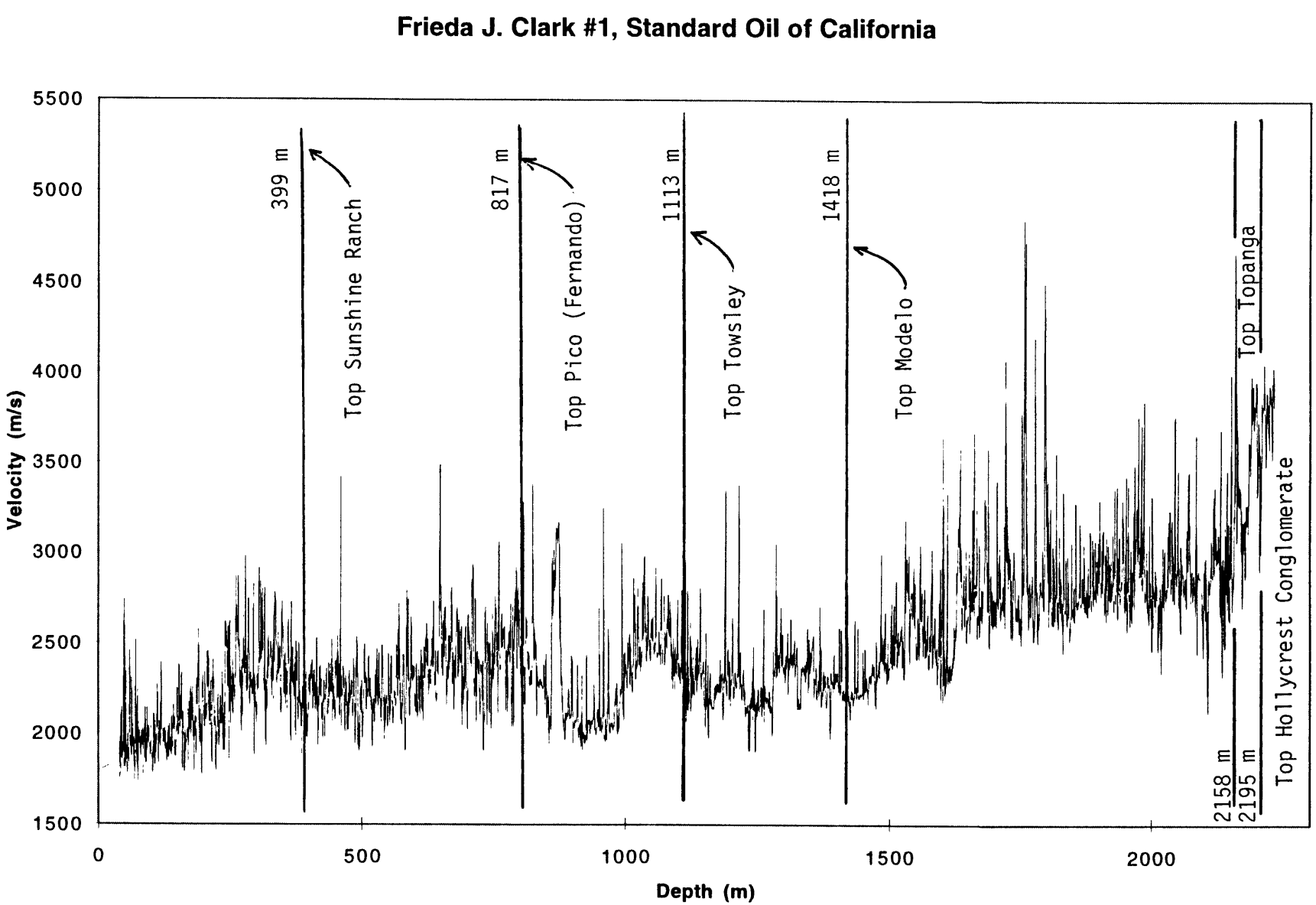
Frieda J. Clark #1, Standard Oil of California
Velocity (m/s)
5500
5000
4500
4000
3500
3000
2500
2000
1500
0
500
1000
1500
2000
Depth (m)
399 m
Top Sunshine Ranch
817 m
Top Pico (Fernando)
1113 m
Top Towsley
1418 m
Top Modelo
2158 m
Top Topanga
2195 m
Top Hollycrest Conglomerate

Figure 11.

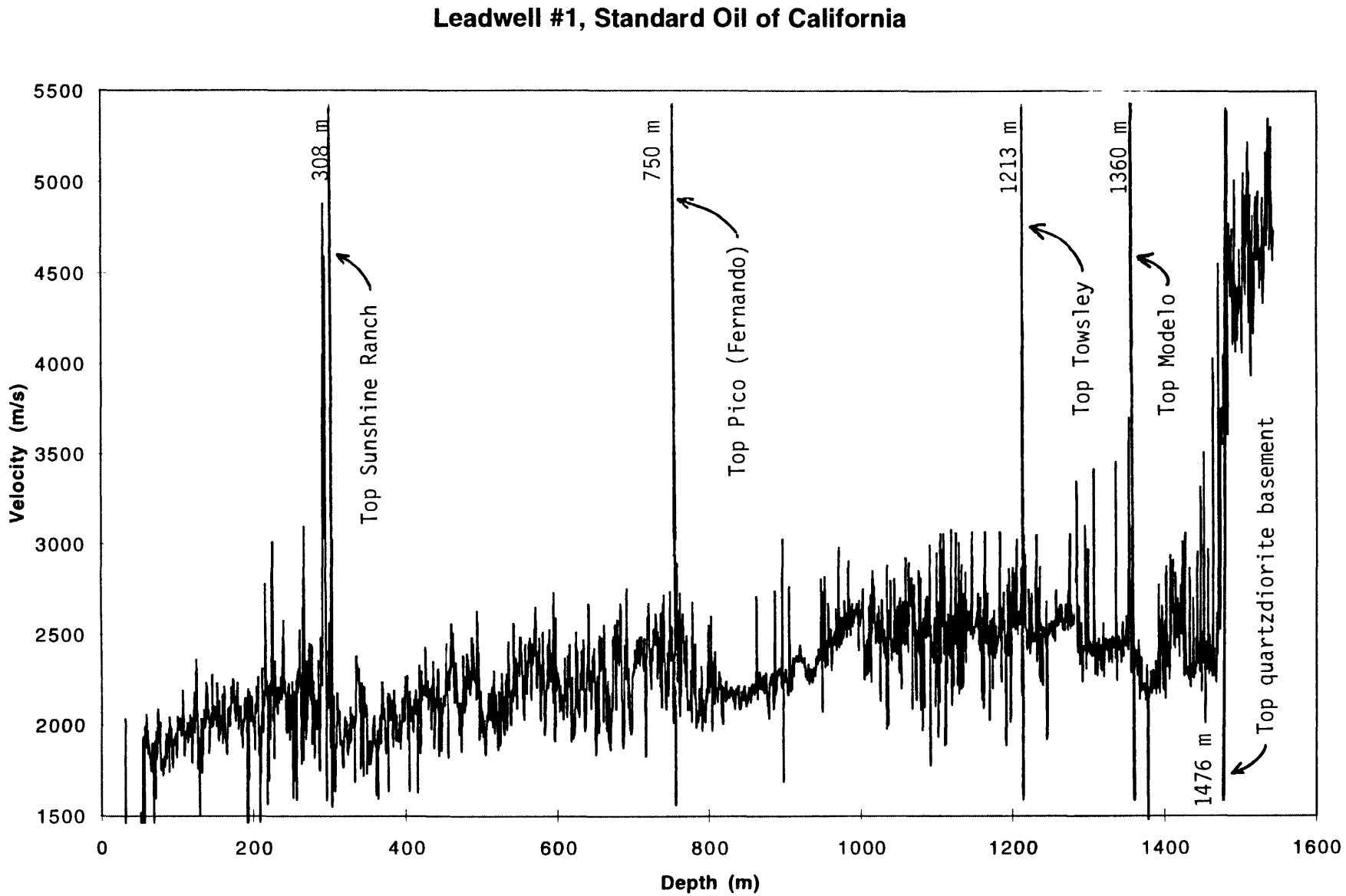
Leadwell #1, Standard Oil of California
Velocity (m/s)
5500
5000
4500
4000
3500
3000
2500
2000
1500
0
200
400
600
800
1000
1200
1400
1600
Depth (m)
308 m
Top Sunshine Ranch
750 m
Top Pico (Fernando)
1213 m
Top Towsley
1360 m
Top Modelo
1476 m
Top quartzdiorite basement

Figure 12.

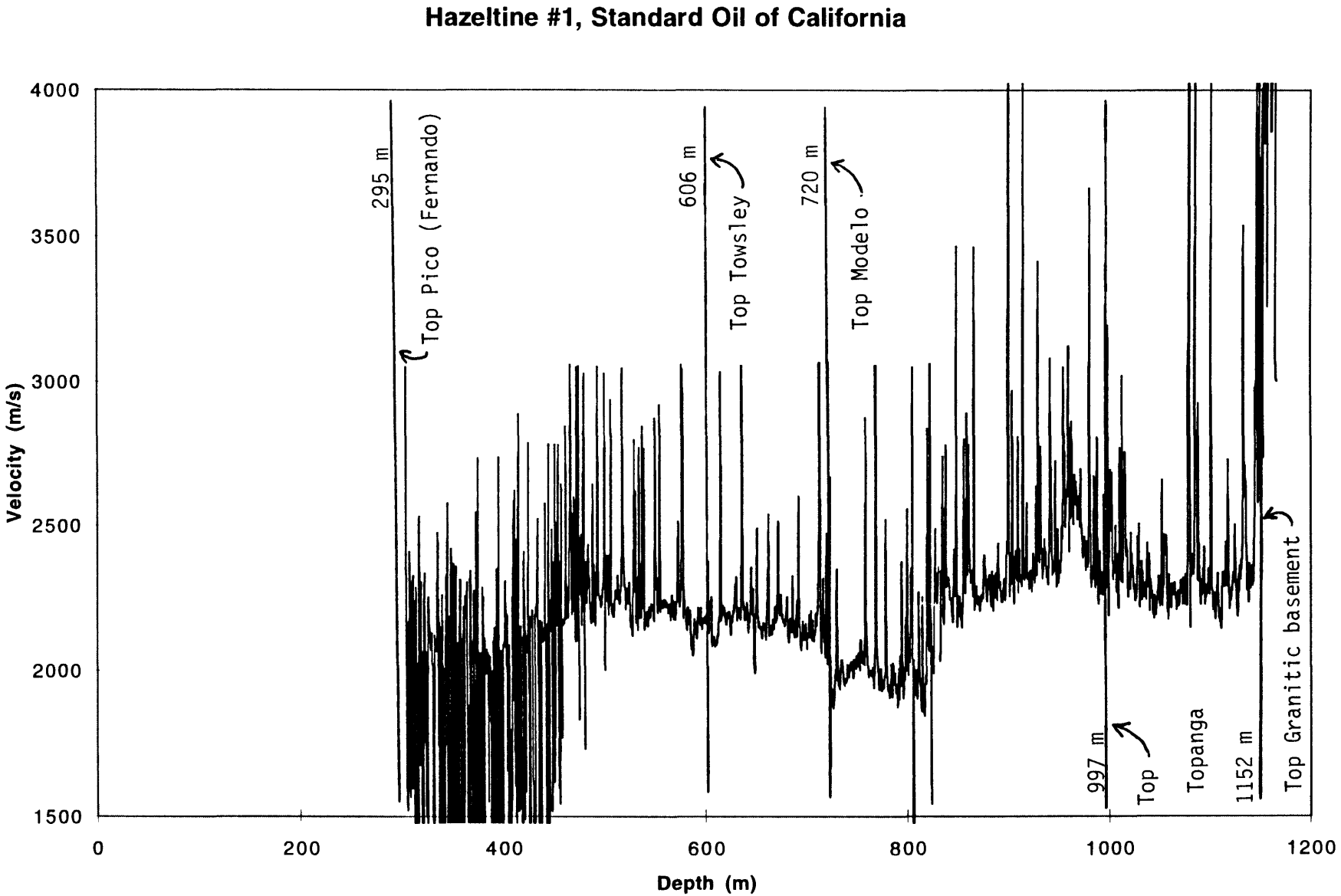
Hazeltine #1, Standard Oil of California
Velocity (m/s)
4000
3500
3000
2500
2000
1500
0
200
400
600
800
1000
1200
Depth (m)
295 m
Top Pico (Fernando)
606 m
Top Towsley
720 m
Top Modelo
997 m
Top
Topanga
1152 m
Top Granitic basement

Figure 13.

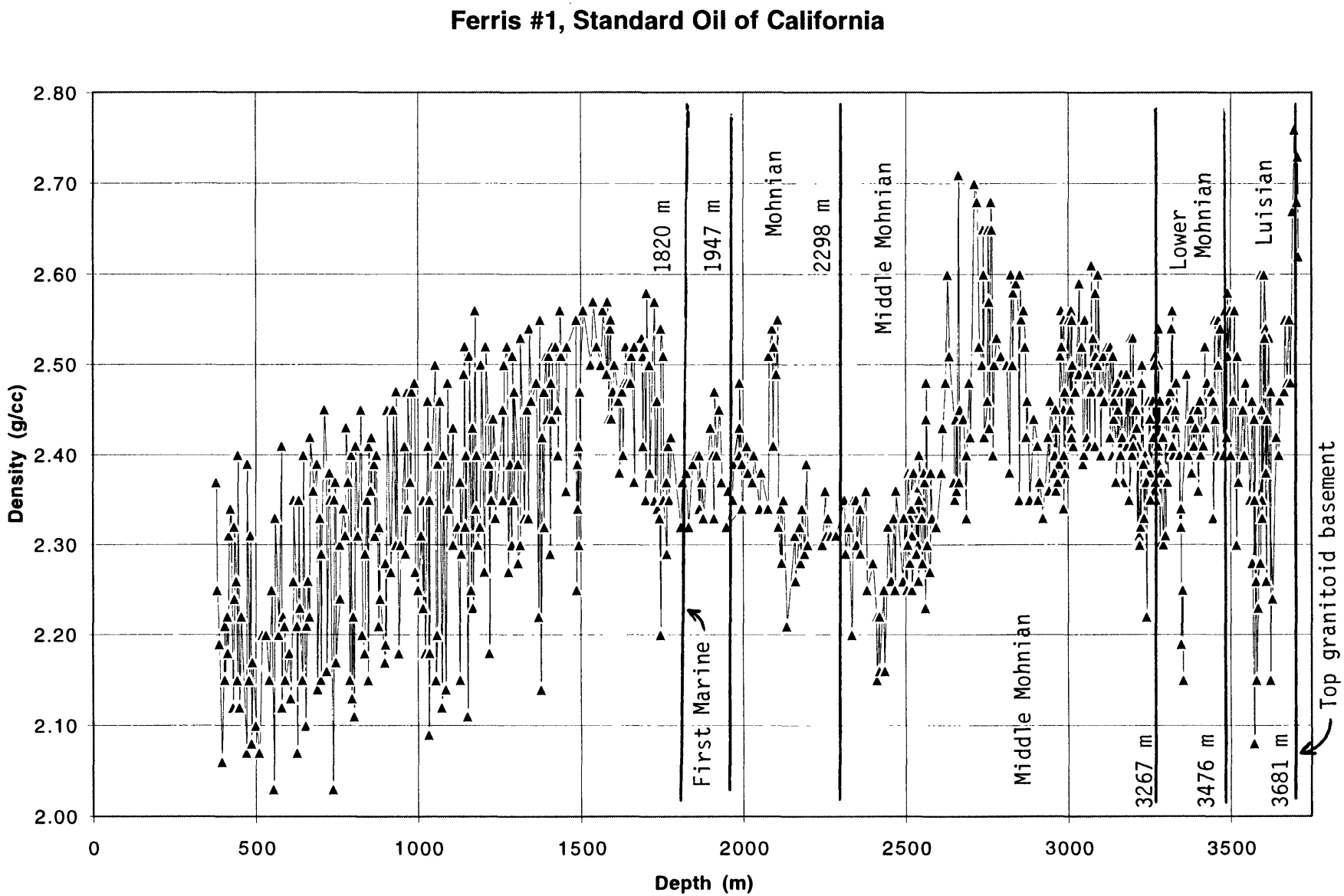
Ferris #1, Standard Oil of California
Density (g/cc)
2.80
2.70
2.60
2.50
2.40
2.30
2.20
2.10
2.00
0
500
1000
1500
2000
2500
3000
3500
Depth (m)
1820 m
1947 m
Mohnian
2298 m
Middle Mohnian
Lower Mohnian
Luisian
First Marine
Middle Mohnian
3267 m
3476 m
3681 m
Top granitoid basement

Figure 14.

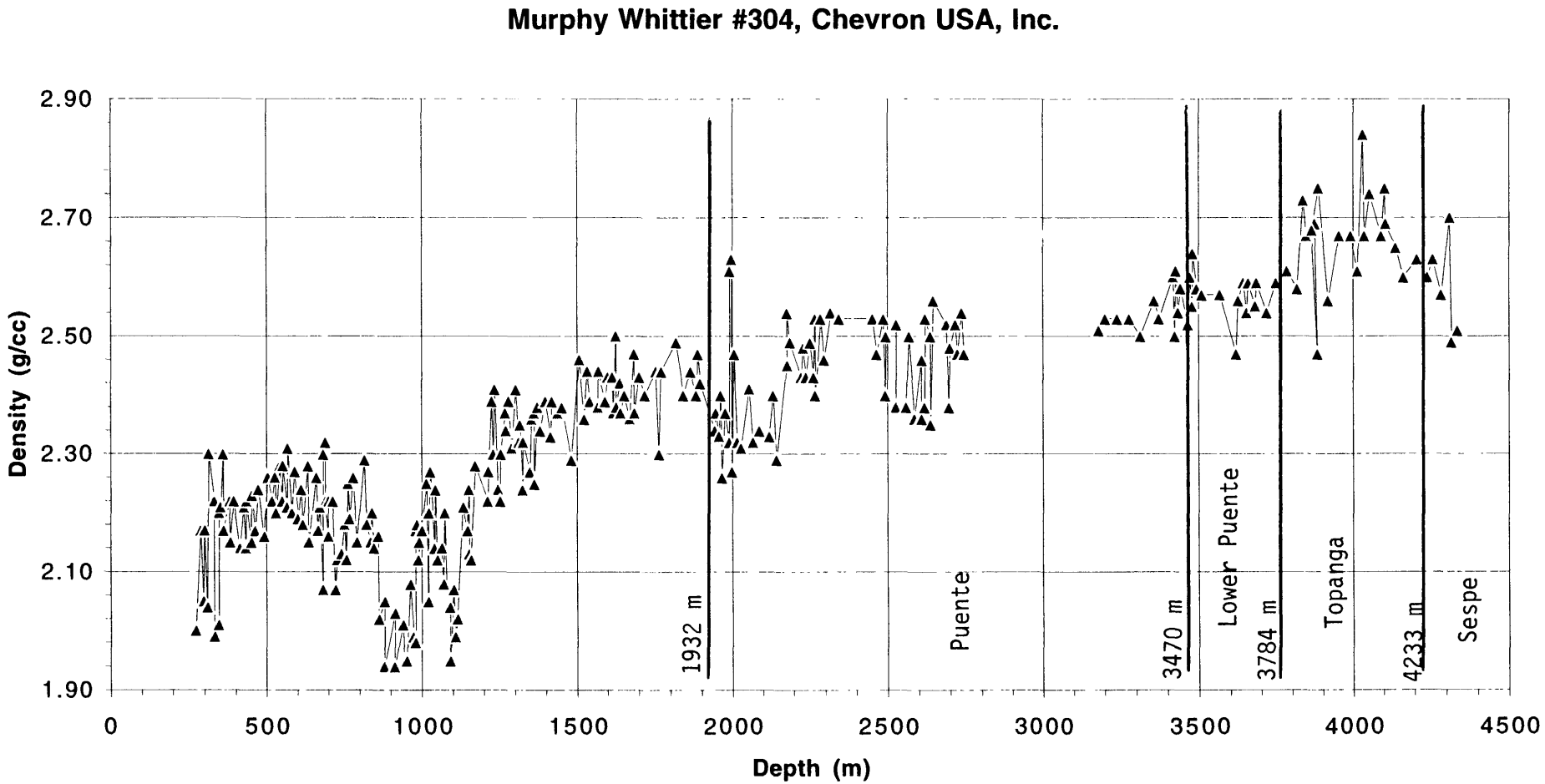
Murphy Whittier #304, Chevron USA, Inc.
Density (g/cc)
2.90
2.70
2.50
2.30
2.10
1.90
0
500
1000
1500
2000
2500
3000
3500
4000
4500
Depth (m)
1932 m
Puente
3470 m
Lower Puente
3784 m
Topanga
4233 m
Sespe

Figure 15.

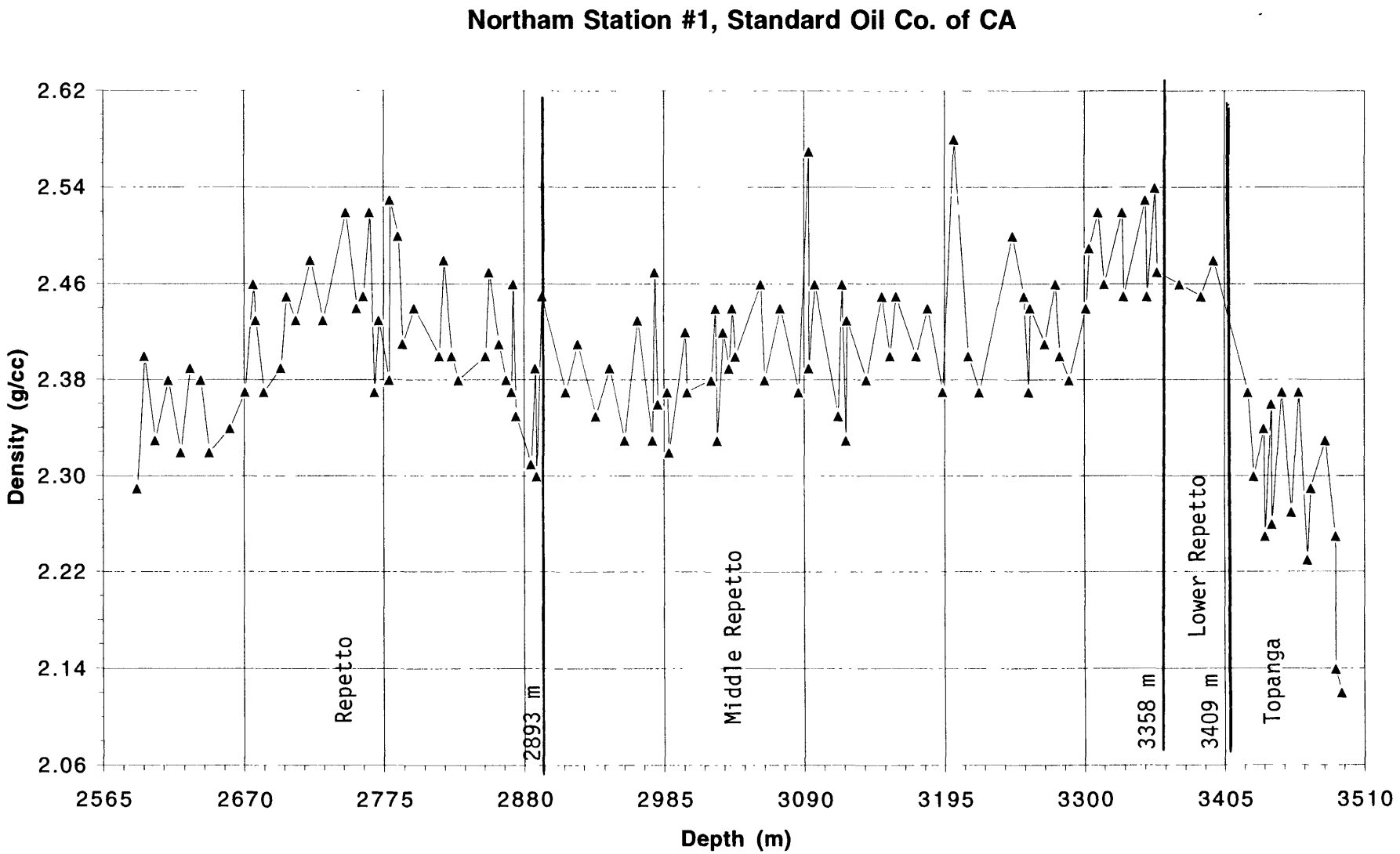
Northam Station #1, Standard Oil Co. of CA
Density (g/cc)
2.62
2.54
2.46
2.38
2.30
2.22
2.14
2.06
2565
2670
2775
2880
2985
3090
3195
3300
3405
3510
Depth (m)
Repetto
2893 m
Middle Repetto
3358 m
Lower Repetto
3409 m
Topanga

Figure 16.

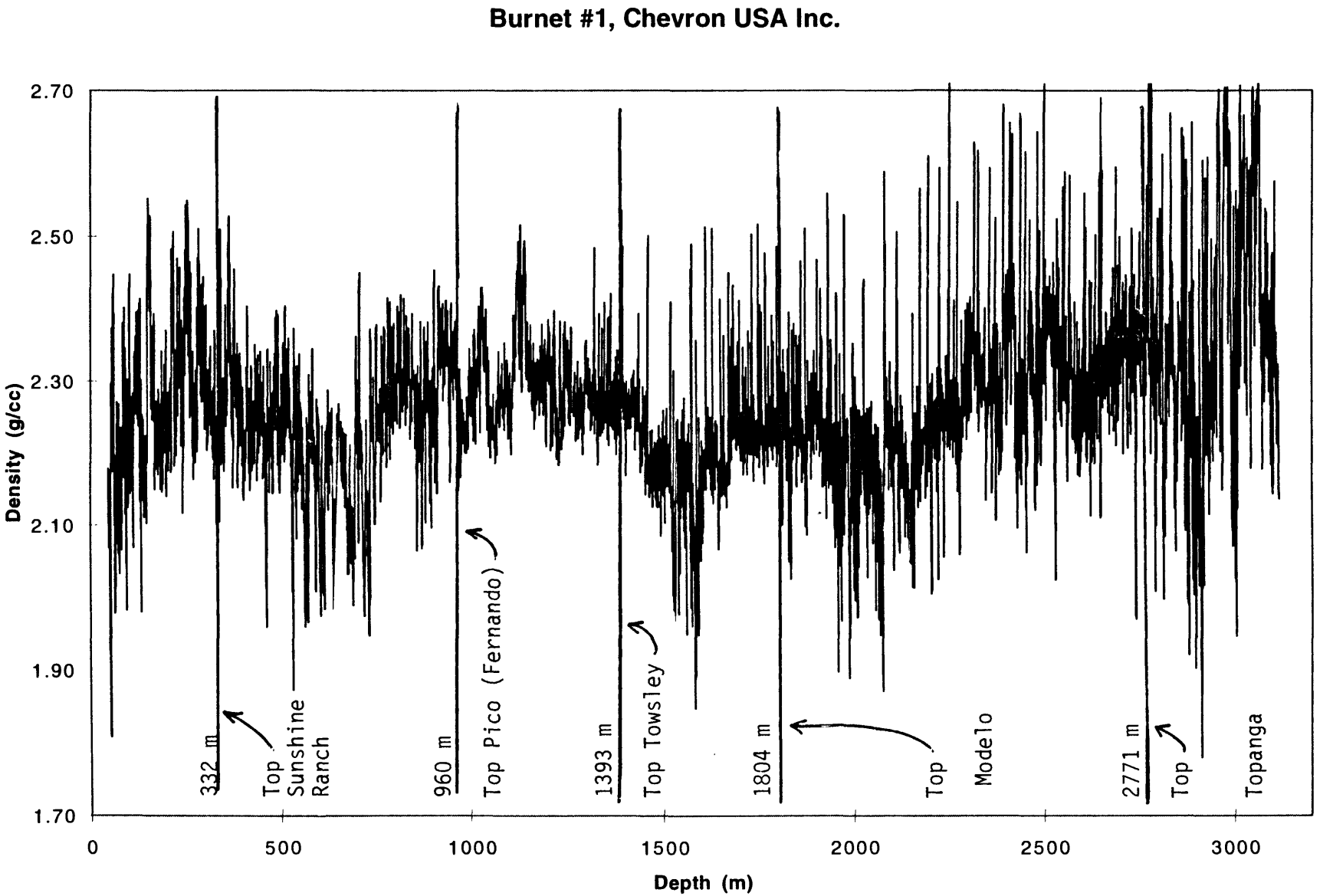
Burnet #1, Chevron USA Inc.
Density (g/cc)
2.70
2.50
2.30
2.10
1.90
1.70
0
500
1000
1500
2000
2500
3000
Depth (m)
332 m
Top Sunshine Ranch
960 m
Top Pico (Fernando)
1393 m
Top Towsley
1804 m
Top Modelo
2771 m
Top Topanga

Figure 17.

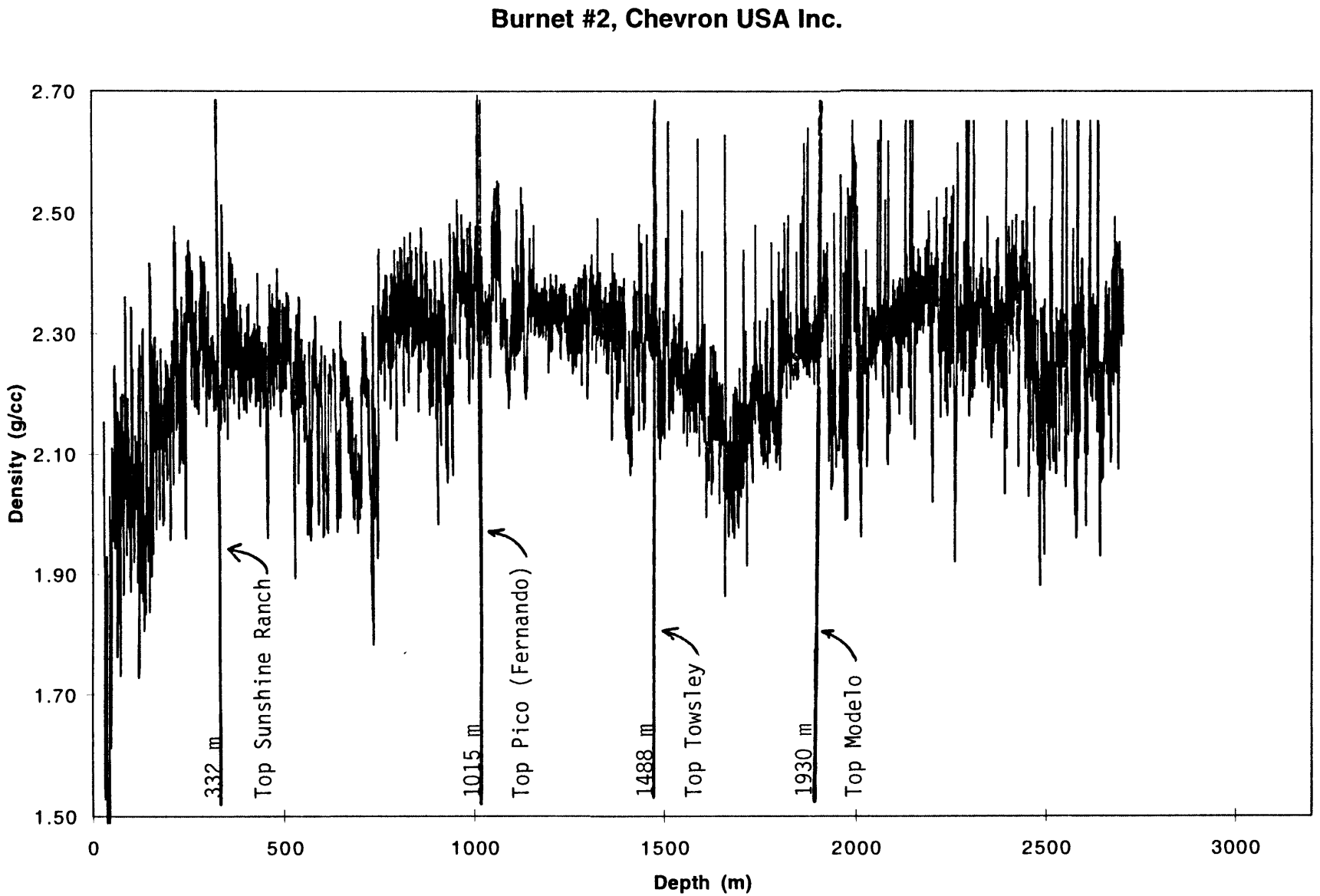
Burnet #2, Chevron USA Inc.
Density (g/cc)
2.70
2.50
2.30
2.10
1.90
1.70
1.50
0
500
1000
1500
2000
2500
3000
Depth (m)
332 m
Top Sunshine Ranch
1015 m
Top Pico (Fernando)
1488 m
Top Towsley
1930 m
Top Modelo

Figure 18.

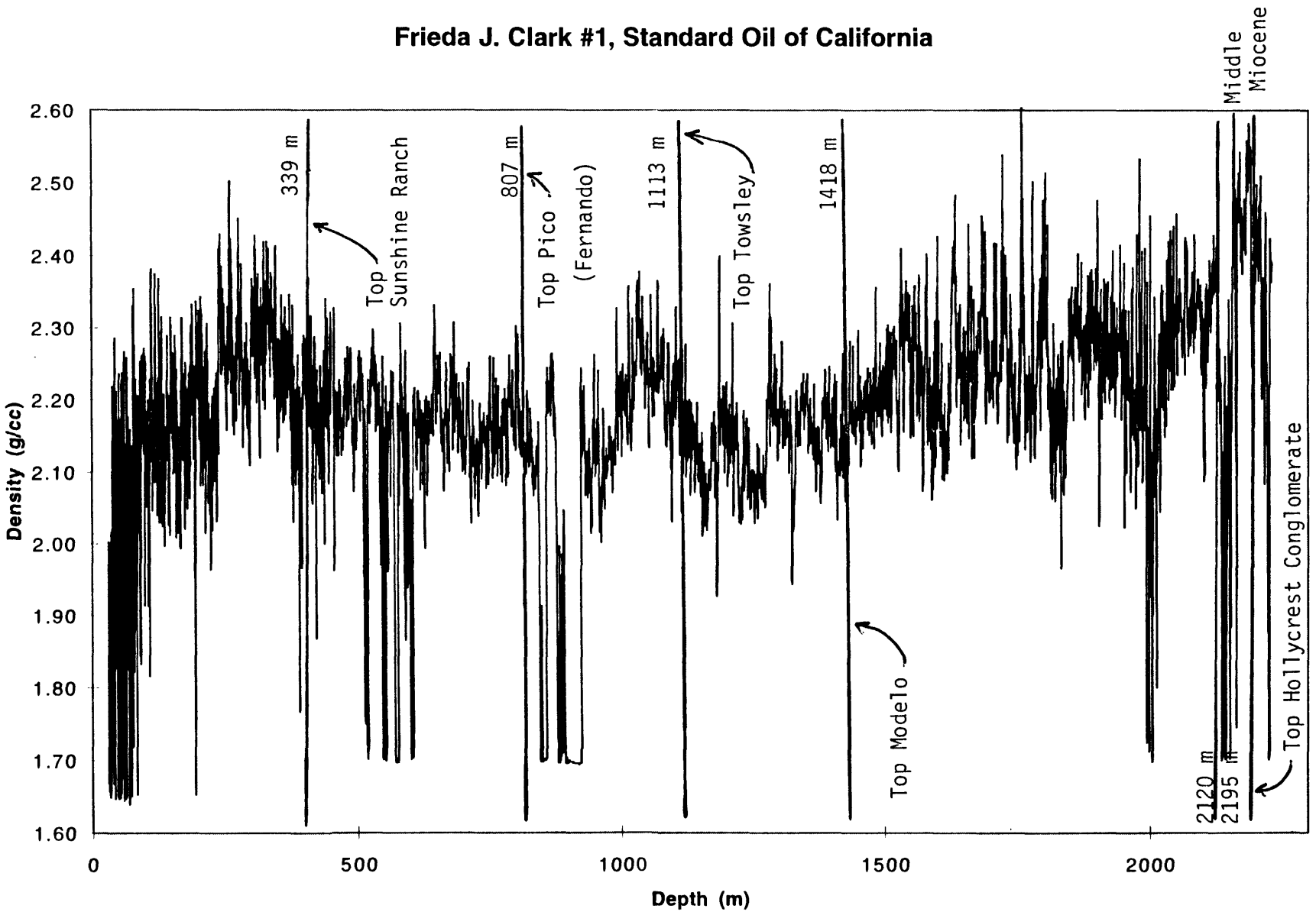
Frieda J. Clark #1, Standard Oil of California
Density (g/cc)
2.60
2.50
2.40
2.30
2.20
2.10
2.00
1.90
1.80
1.70
1.60
0
500
1000
1500
2000
Depth (m)
339 m
Top Sunshine Ranch
807 m
Top Pico
(Fernando)
1113 m
Top Towsley
1418 m
Top Modelo
2120 m
2195 m
Middle Miocene
Top Hollycrest Conglomerate

Figure 19.

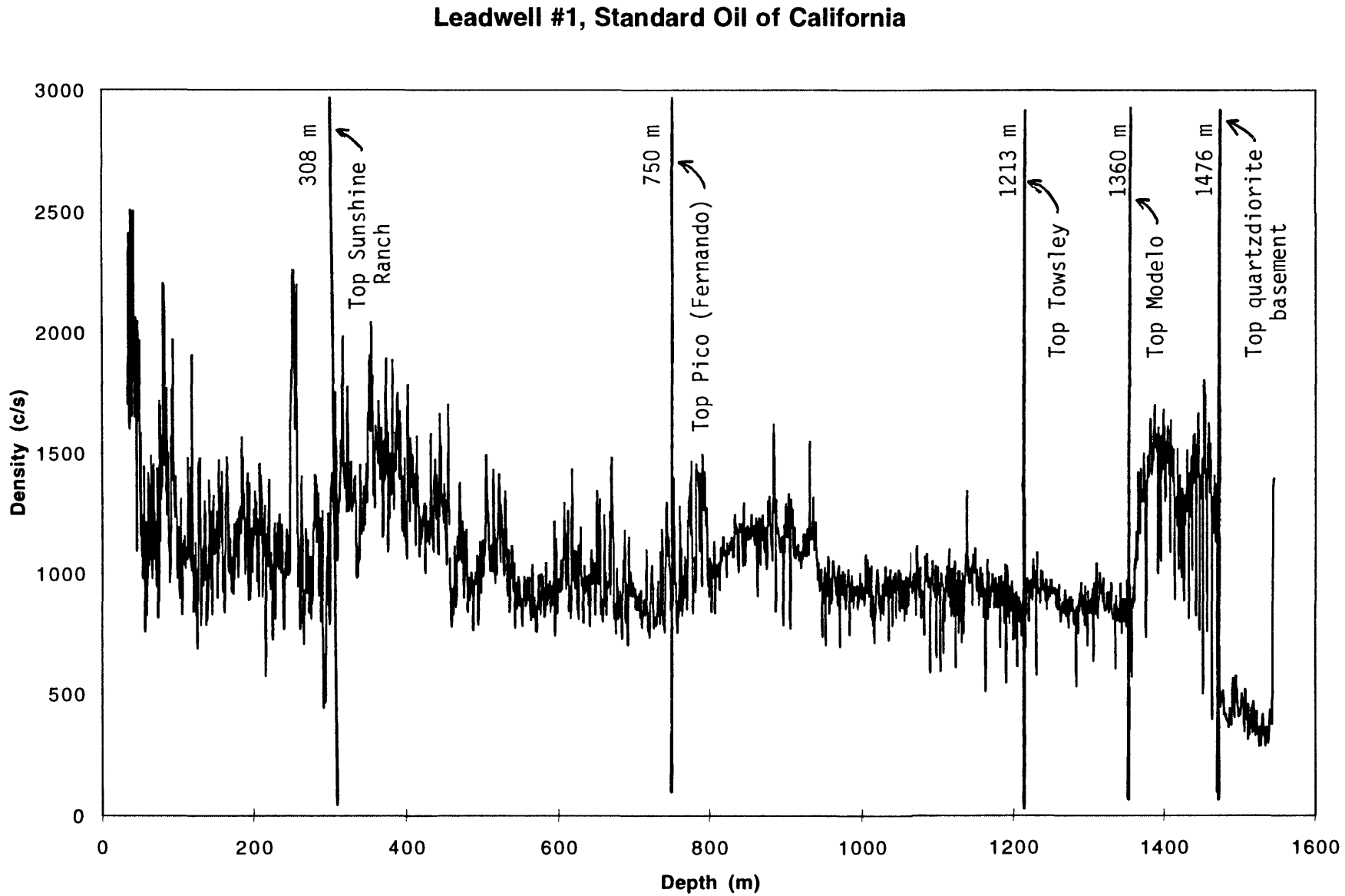
Leadwell #1, Standard Oil of California
Density (c/s)
3000
2500
2000
1500
1000
500
0
0
200
400
600
800
1000
1200
1400
1600
Depth (m)
308 m
Top Sunshine Ranch
750 m
Top Pico (Fernando)
1213 m
Top Towsley
1360 m
Top Modelo
1476 m
Top quartzdiorite basement

Figure 20.

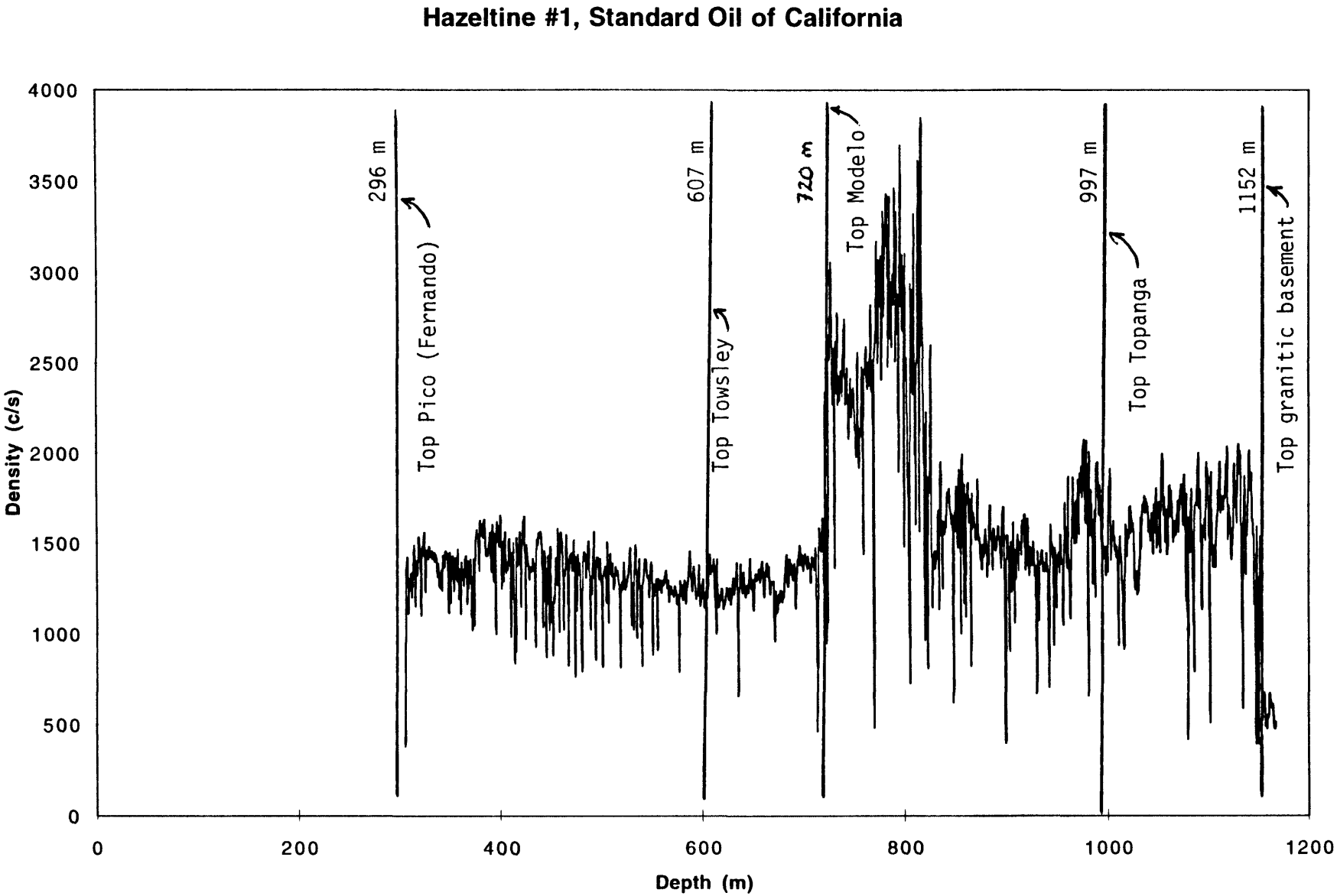
Hazeltine #1, Standard Oil of California
Density (c/s)
4000
3500
3000
2500
2000
1500
1000
500
0
0
200
400
600
800
1000
1200
Depth (m)
296 m
Top Pico (Fernando)
607 m
Top Towsley
720 m
Top Modelo
997 m
Top Topanga
1152 m
Top granitic basement

Figure 21.

SAN FERNANDO VALLEY WELLS
SYNTHETIC SEISMOGRAMS
BURN1, BURN2, BURN1+2, FRIEDA, HAZEL, LEADWELL

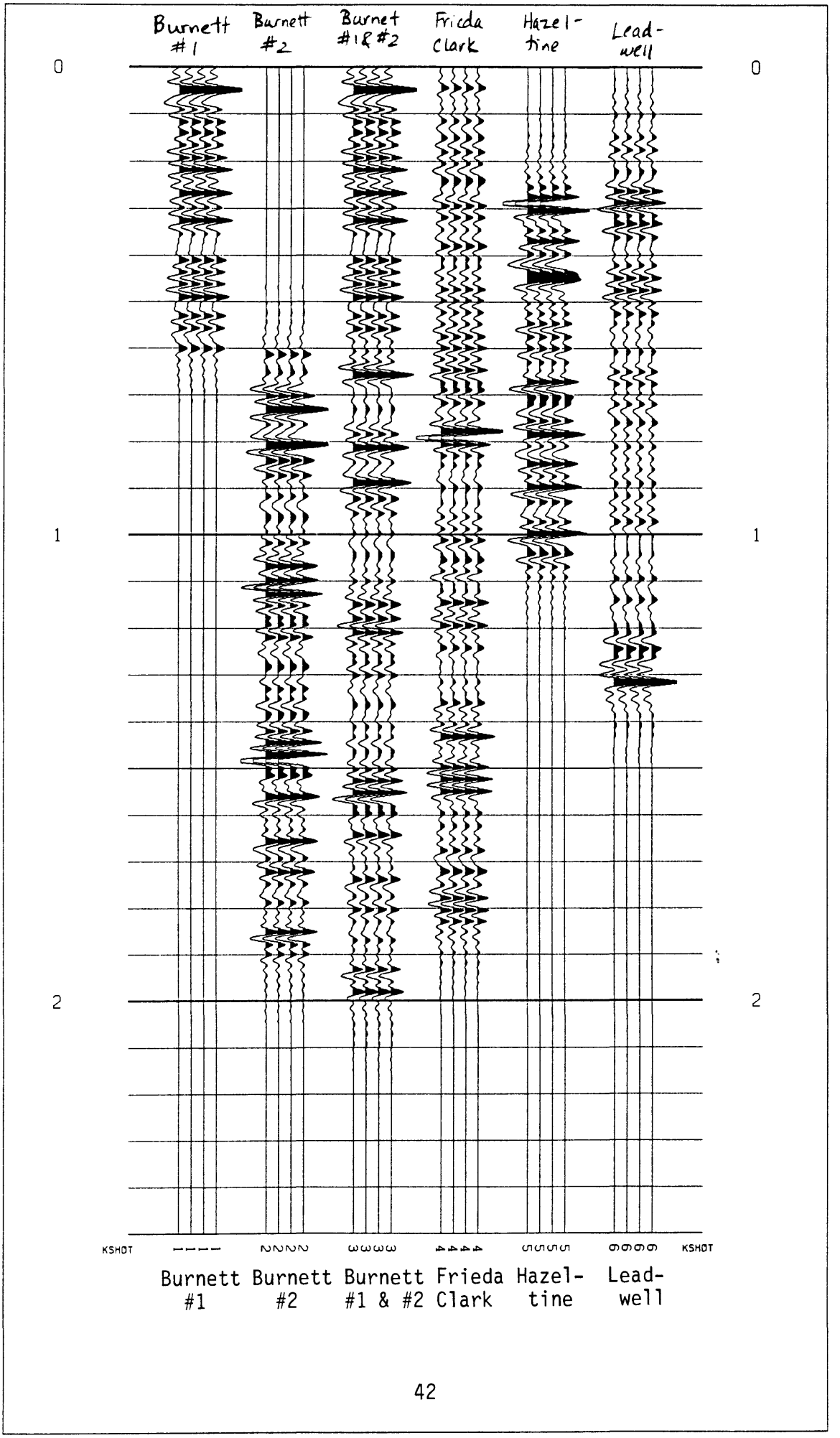

Figure 22.

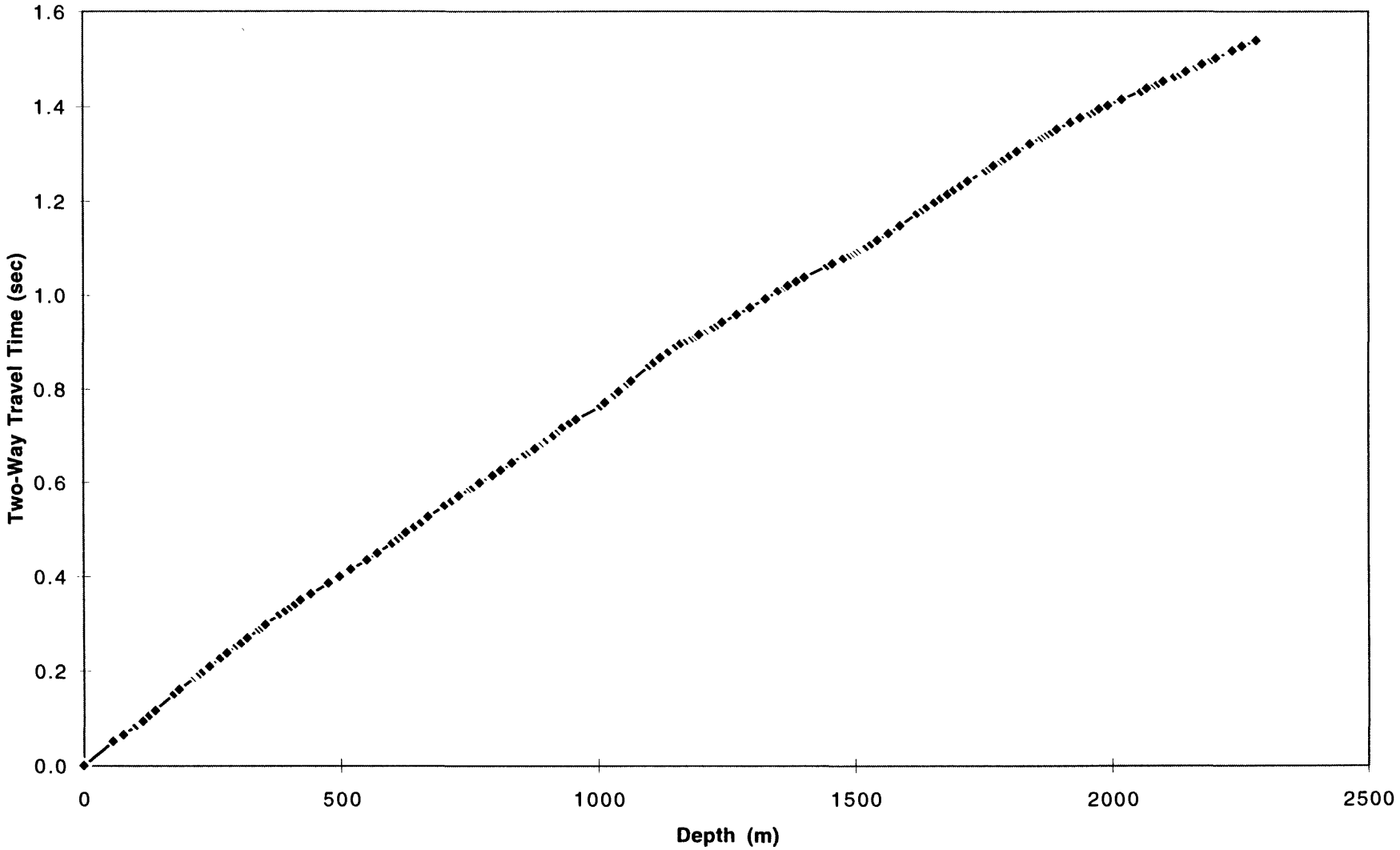
Consolidated Rock Products #1, Irwindale
Two-Way Travel Time (sec)
1.6
1.4
1.2
1.0
0.8
0.6
0.4
0.2
0.0
0
500
1000
1500
2000
2500
Depth (m)

Figure 23.

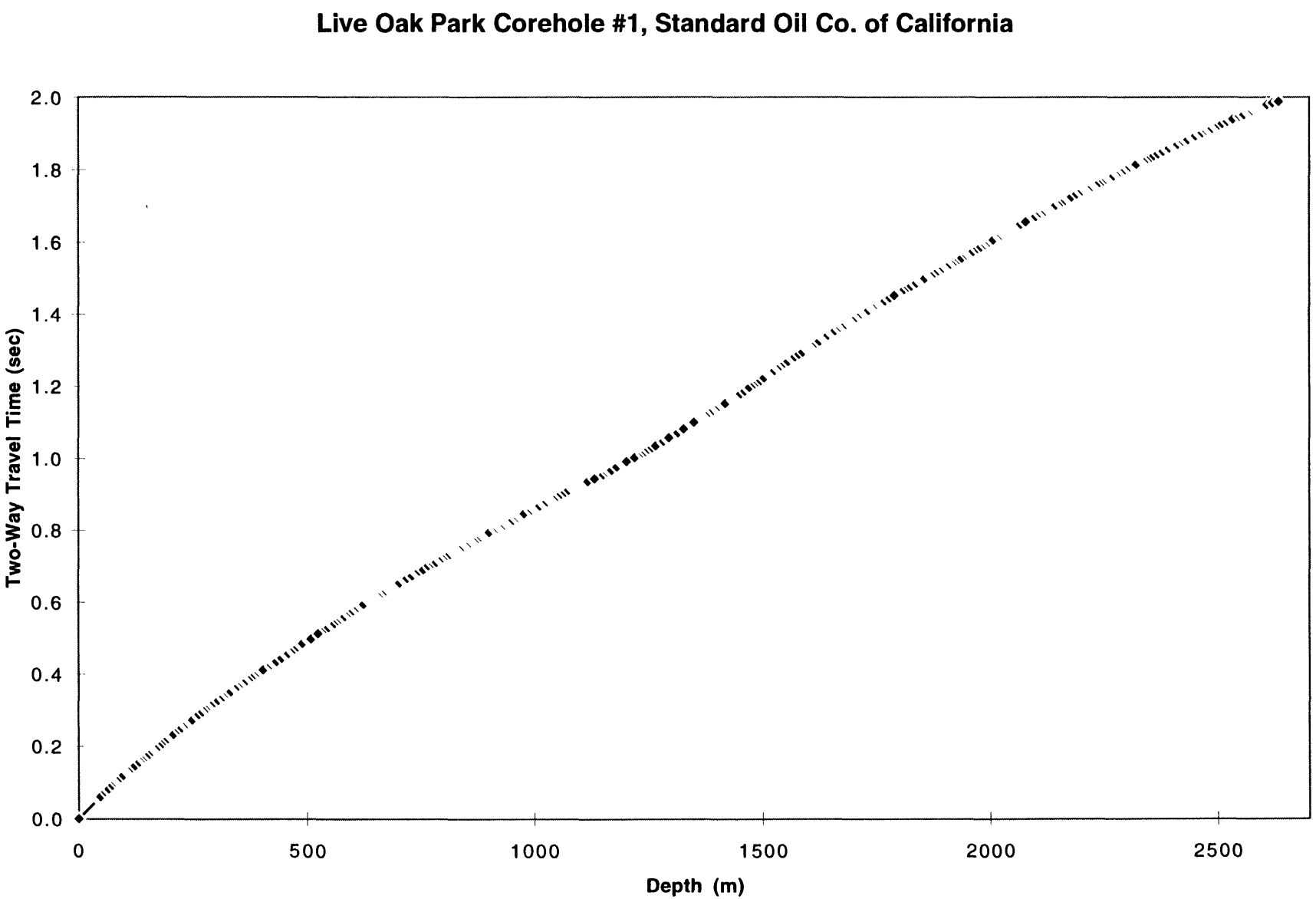
Live Oak Park Corehole #1, Standard Oil Co. of California
Two-Way Travel Time (sec)
2.0
1.8
1.6
1.4
1.2
1.0
0.8
0.6
0.4
0.2
0.0
0
500
1000
1500
2000
2500
Depth (m)

Figure 24.

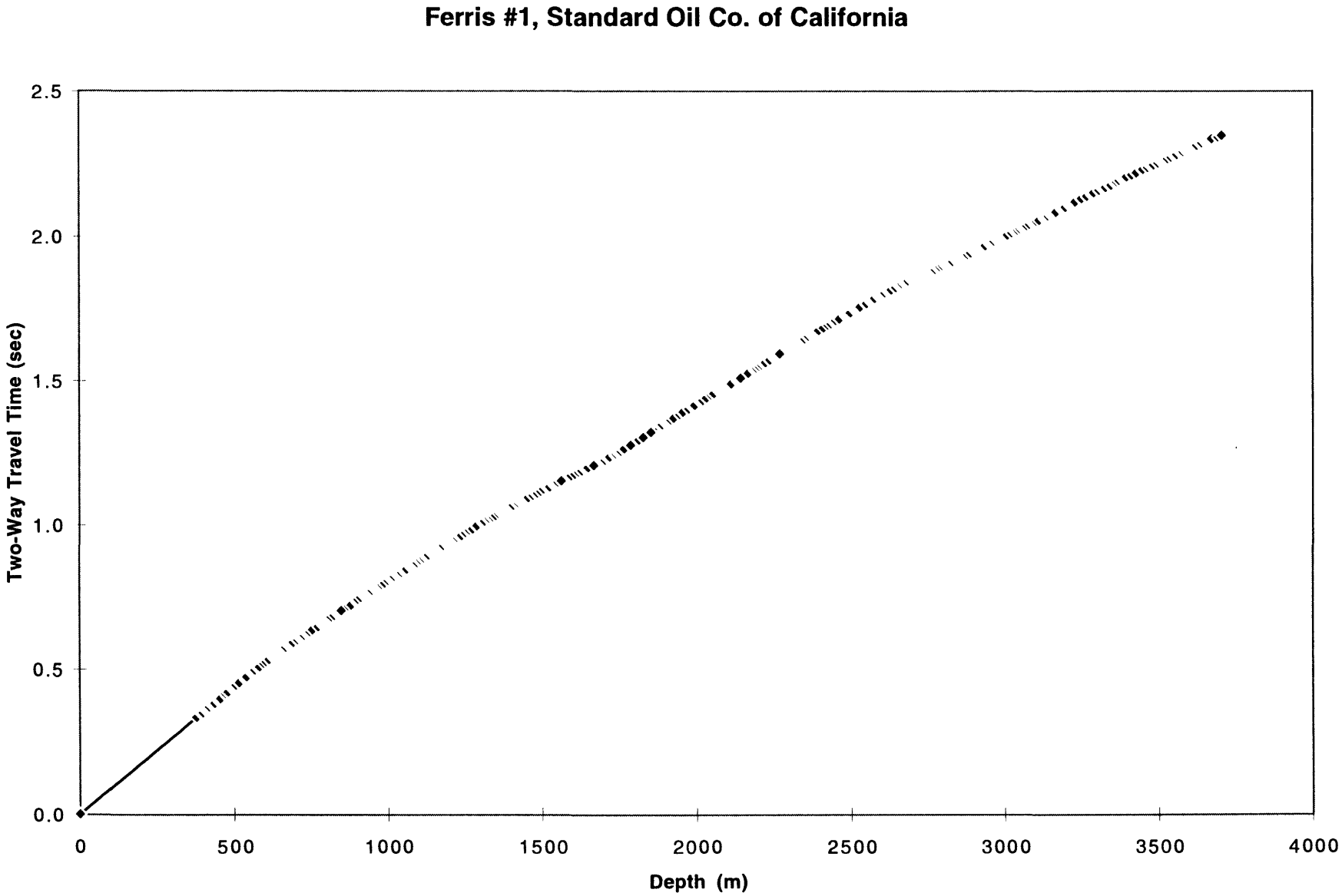
Ferris #1, Standard Oil Co. of California
Two-Way Travel Time (sec)
2.5
2.0
1.5
1.0
0.5
0.0
0
500
1000
1500
2000
2500
3000
3500
4000
Depth (m)

Figure 25.

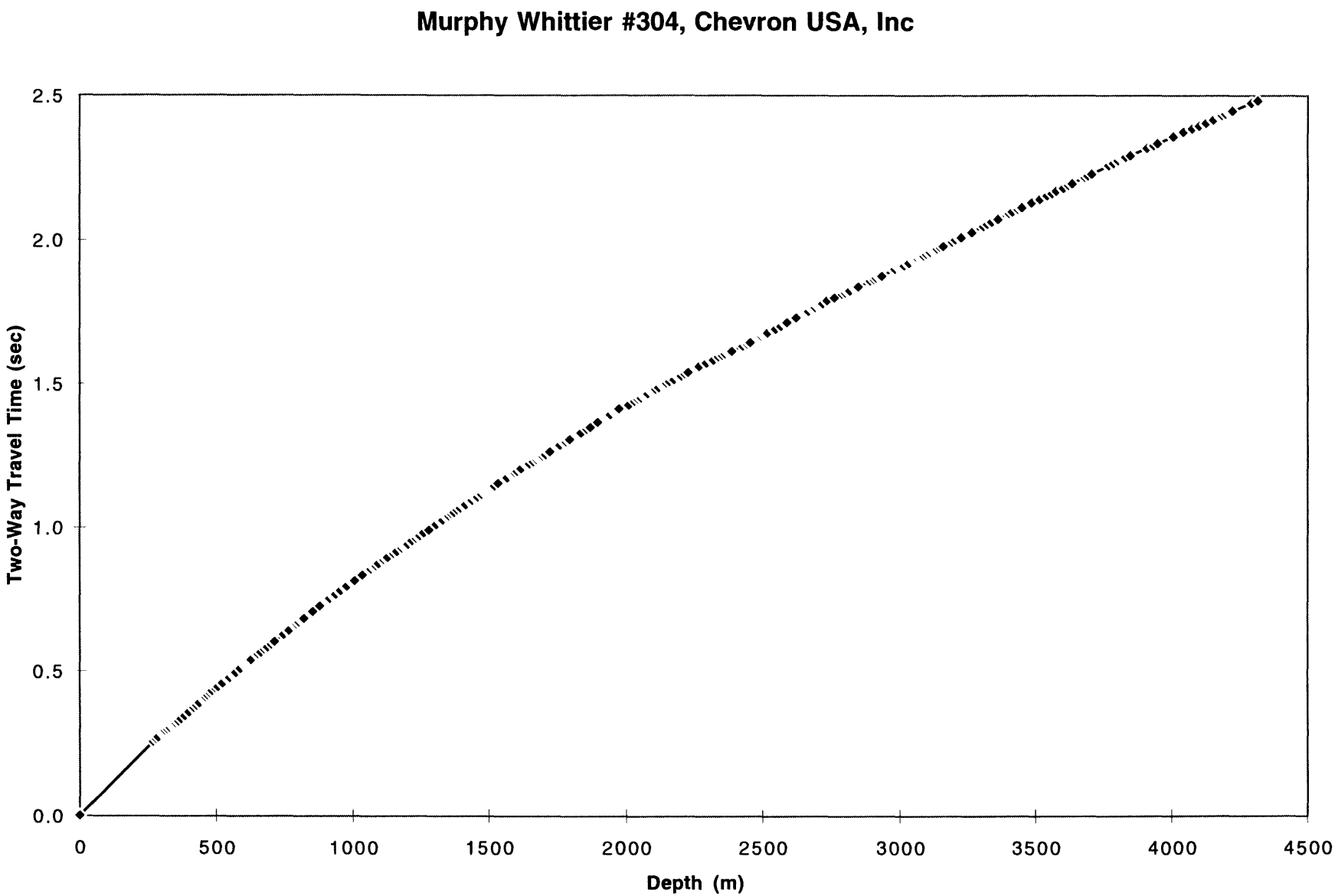
Murphy Whittier #304, Chevron USA, Inc
Two-Way Travel Time (sec)
2.5
2.0
1.5
1.0
0.5
0.0
0
500
1000
1500
2000
2500
3000
3500
4000
4500
Depth (m)

Figure 26.

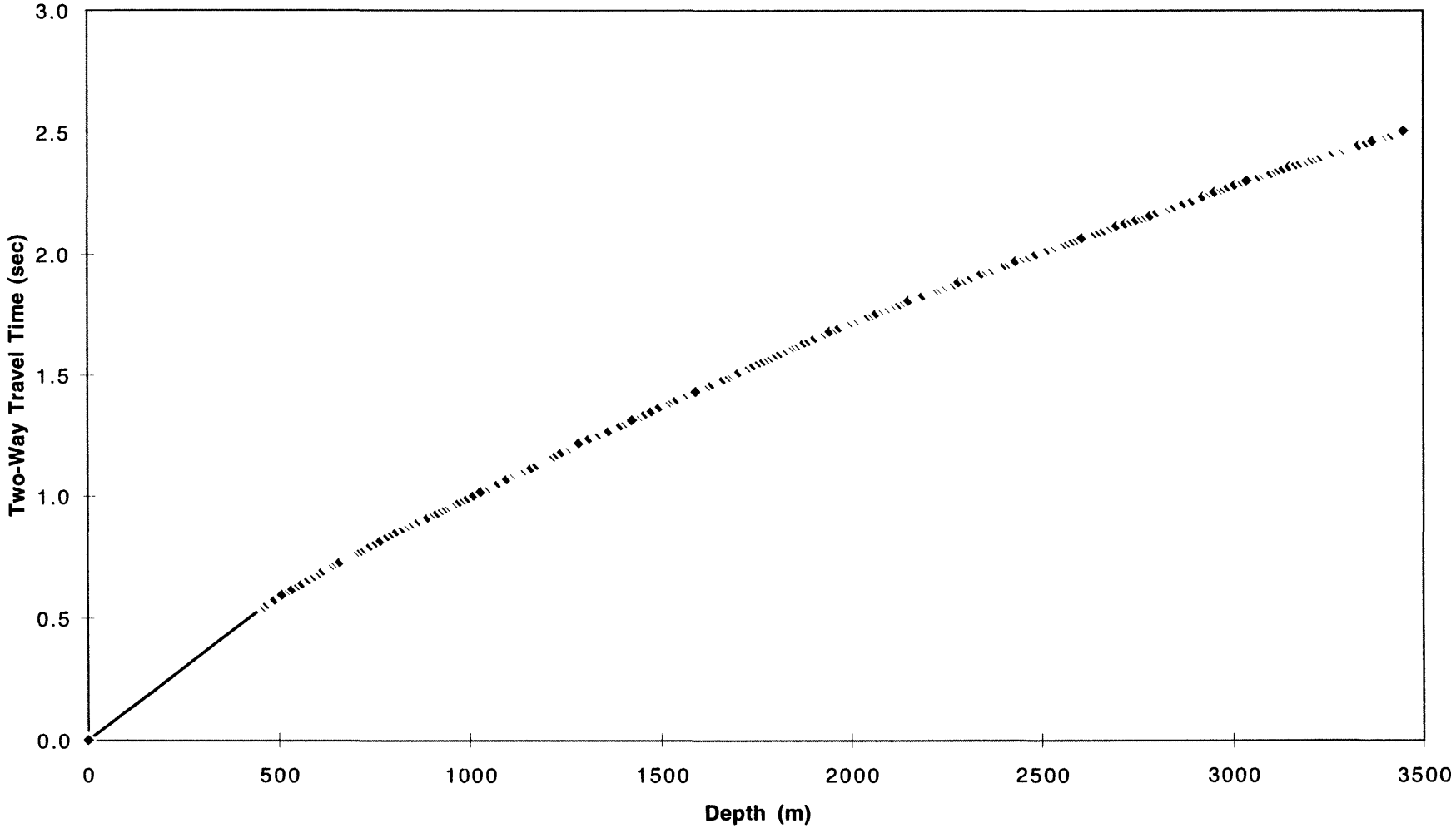
Northam Station Core Hole #1, Standard Oil Co. of California
Two-Way Travel Time (sec)
3.0
2.5
2.0
1.5
1.0
0.5
0.0
0
500
1000
1500
2000
2500
3000
3500
Depth (m)

Figure 27.

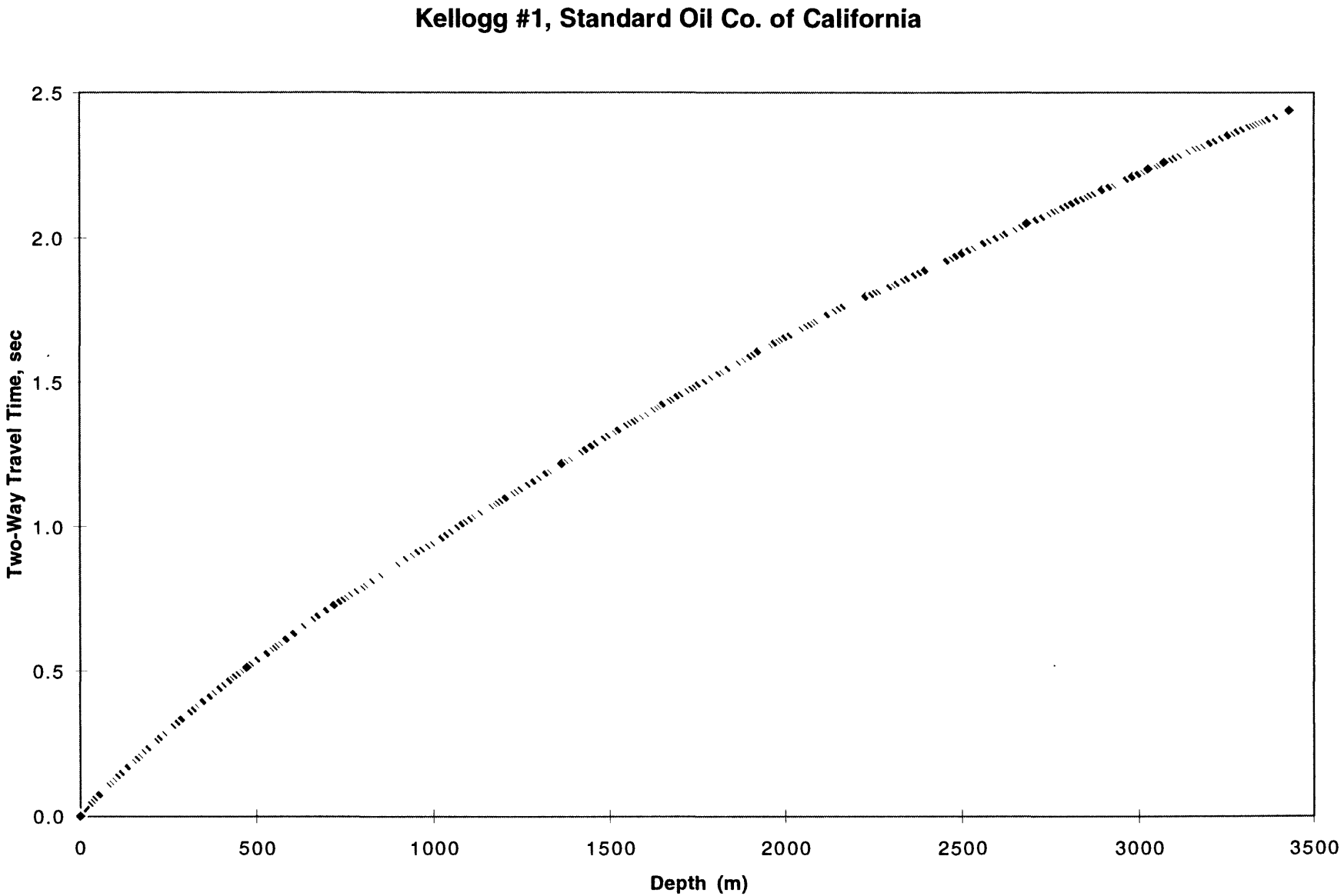
Kellogg #1, Standard Oil Co. of California
Two-Way Travel Time, sec
2.5
2.0
1.5
1.0
0.5
0.0
0
500
1000
1500
2000
2500
3000
3500
Depth (m)

Figure 28.

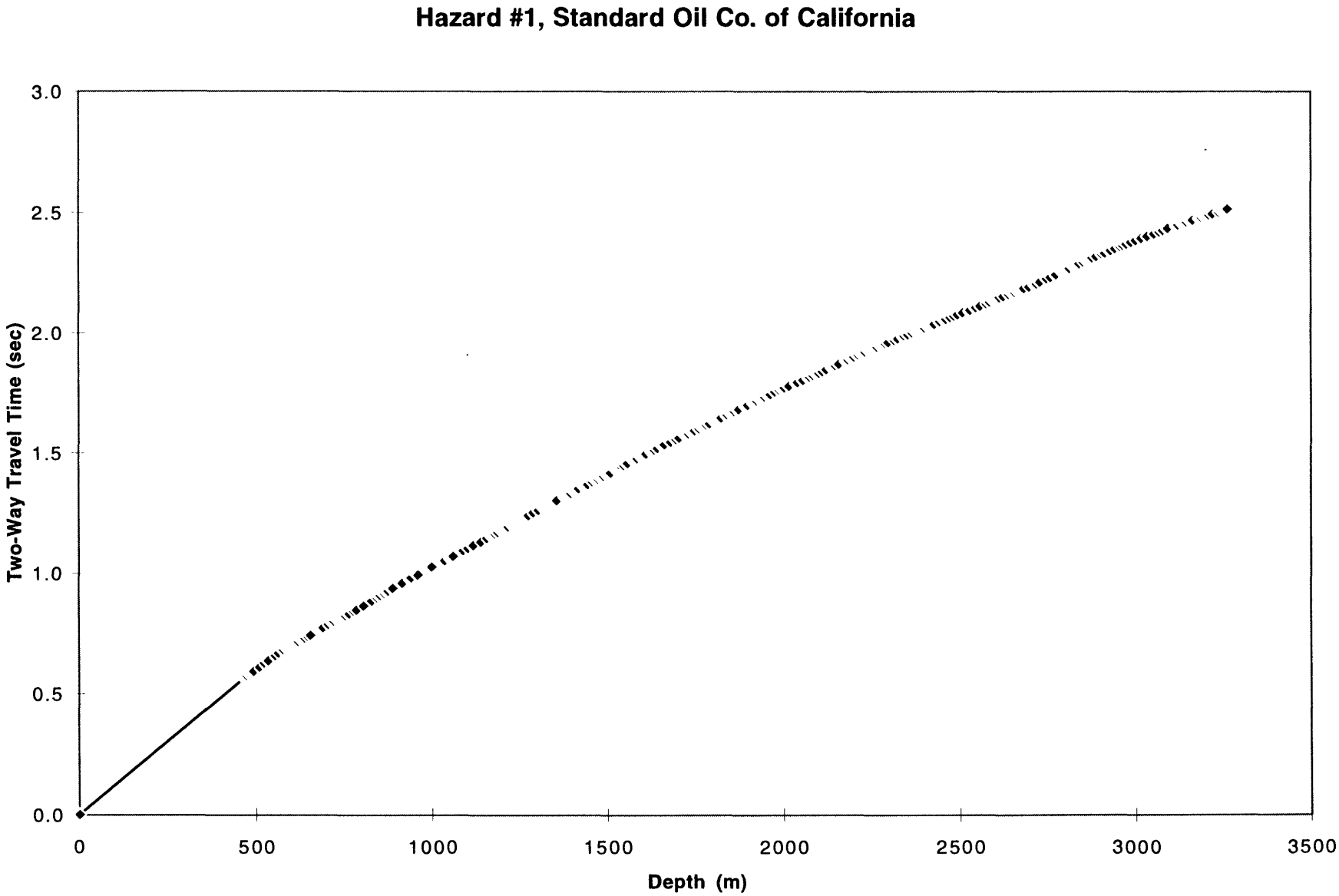
Hazard #1, Standard Oil Co. of California
Two-Way Travel Time (sec)
3.0
2.5
2.0
1.5
1.0
0.5
0.0
0
500
1000
1500
2000
2500
3000
3500
Depth (m)

Figure 29.

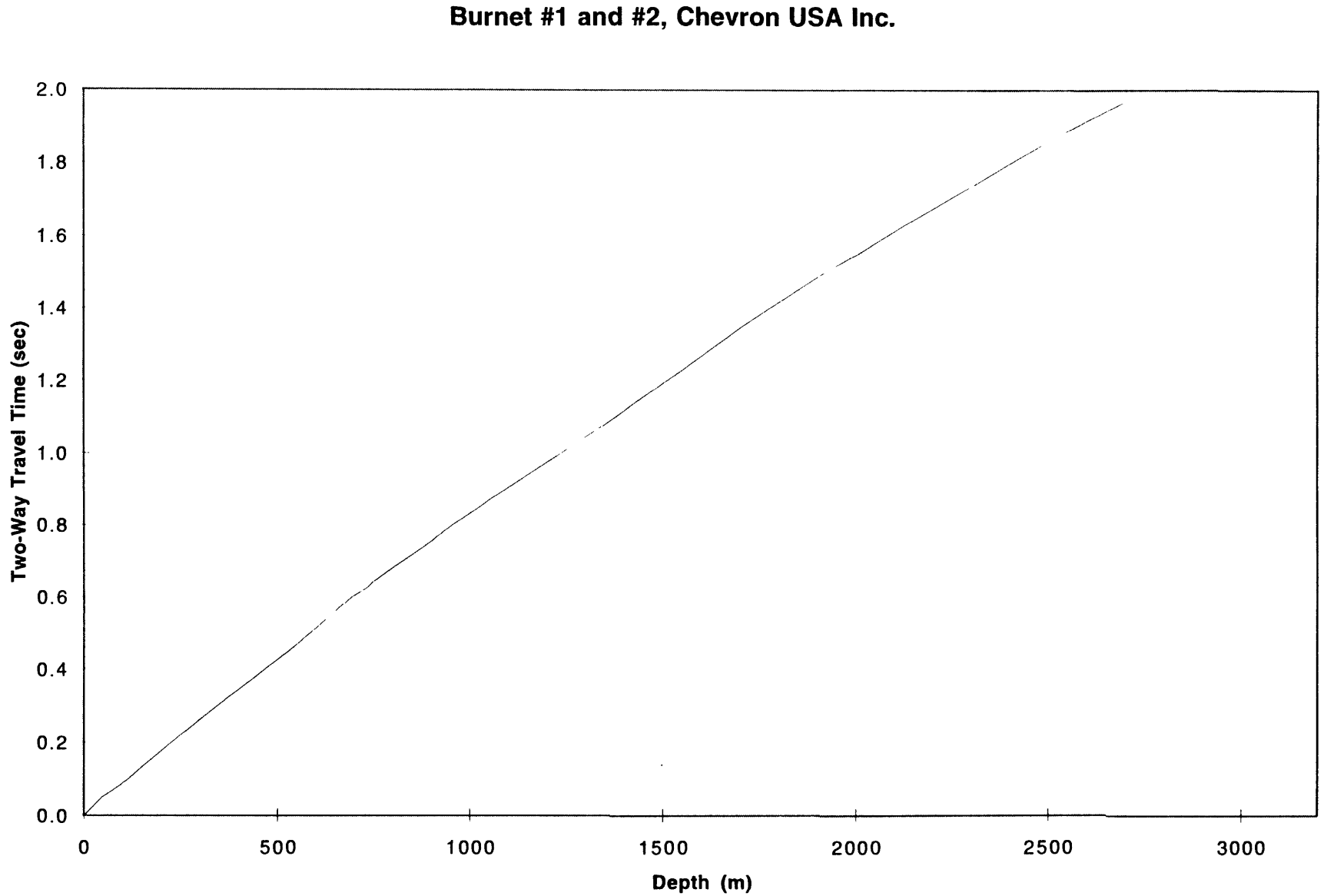
Burnet #1 and #2, Chevron USA Inc.
Two-Way Travel Time (sec)
2.0
1.8
1.6
1.4
1.2
1.0
0.8
0.6
0.4
0.2
0.0
0
500
1000
1500
2000
2500
3000
Depth (m)

Figure 30.

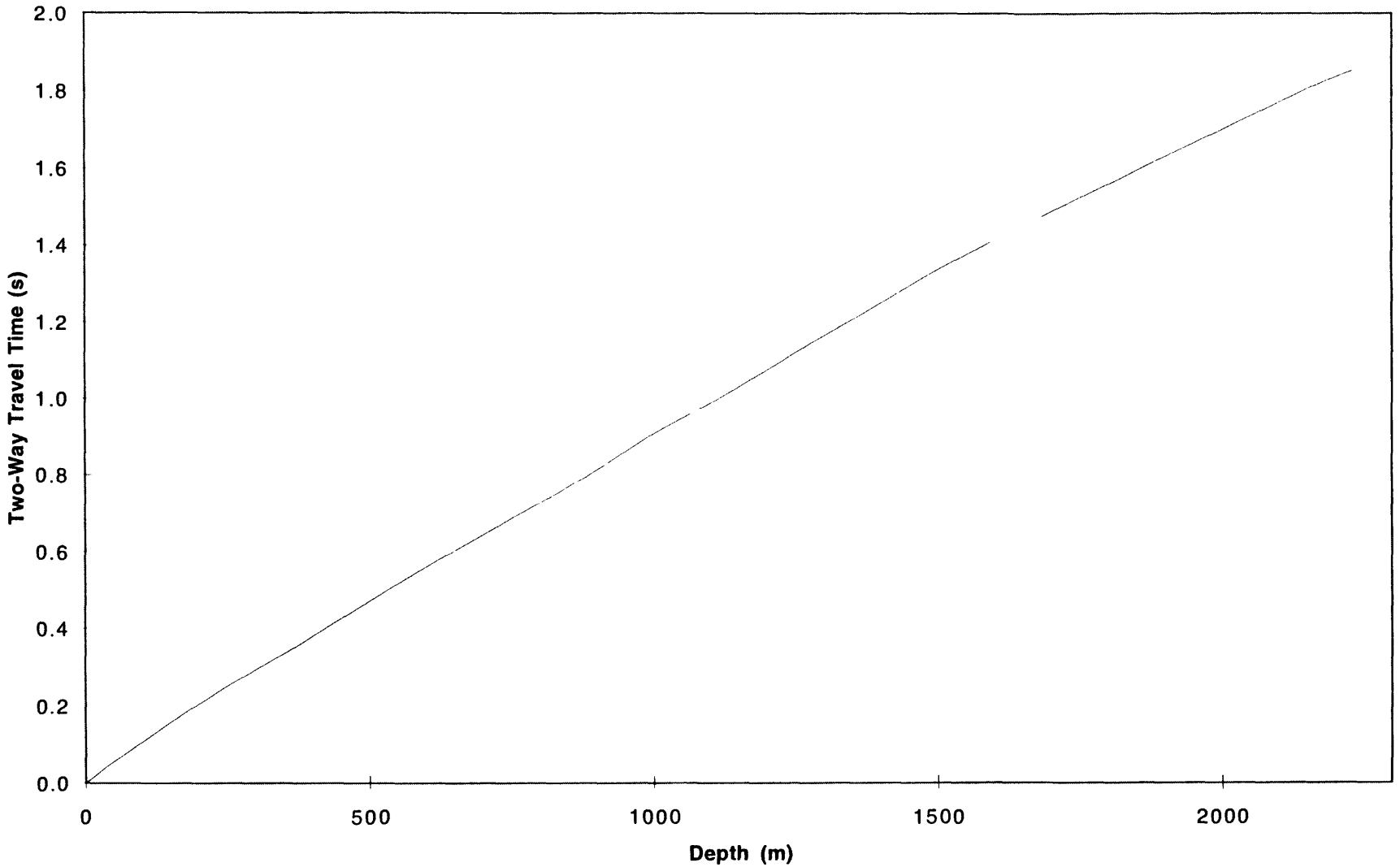
Frieda J. Clark #1, Standard Oil of California
Two-Way Travel Time (s)
2.0
1.8
1.6
1.4
1.2
1.0
0.8
0.6
0.4
0.2
0.0
0
500
1000
1500
2000
Depth (m)

Figure 31.

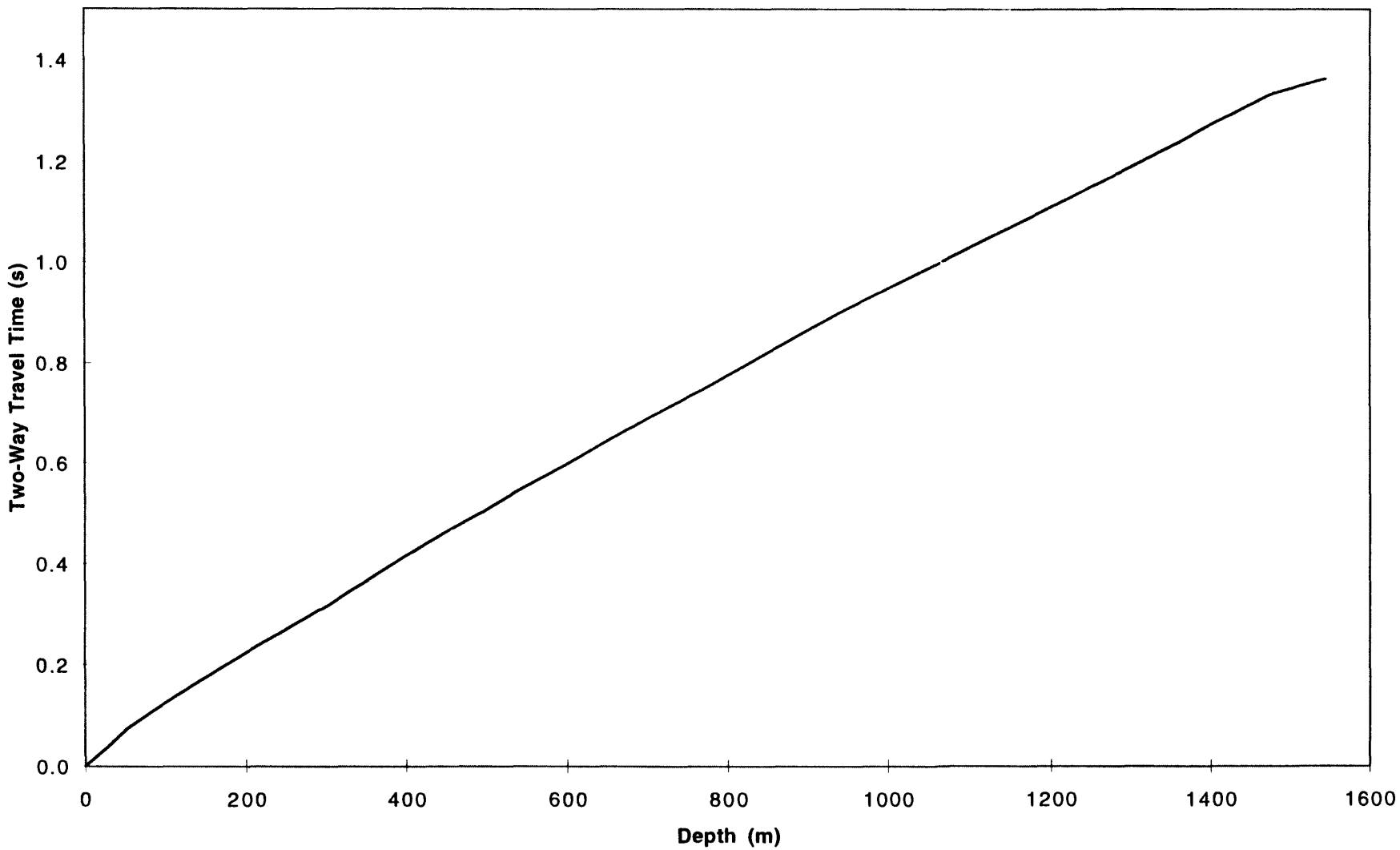
Leadwell #1, Standard Oil of California
Two-Way Travel Time (s)
1.4
1.2
1.0
0.8
0.6
0.4
0.2
0.0
0
200
400
600
800
1000
1200
1400
1600
Depth (m)

Figure 32.

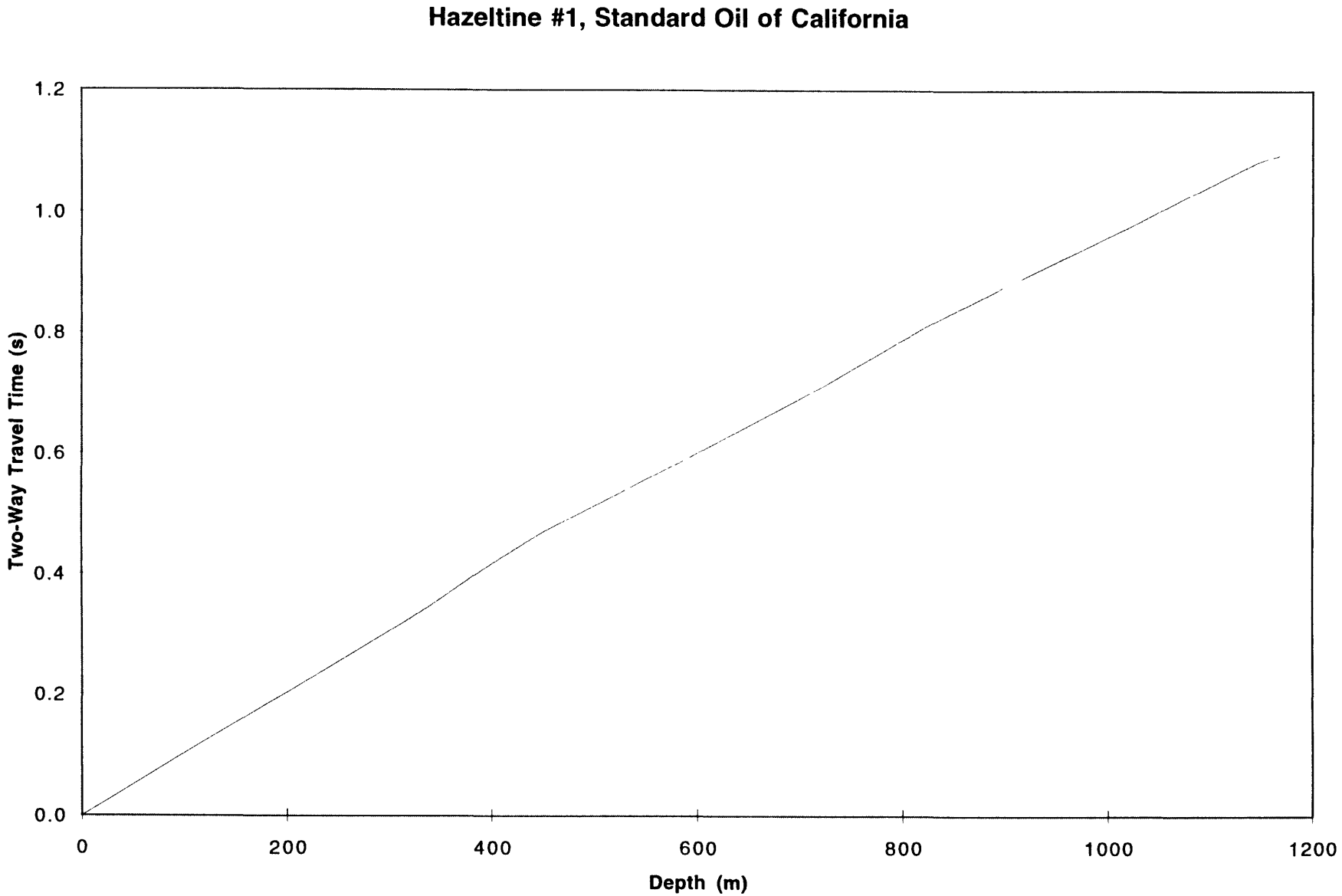
Hazeltine #1, Standard Oil of California
Two-Way Travel Time (s)
1.2
1.0
0.8
0.6
0.4
0.2
0.0
0
200
400
600
800
1000
1200
Depth (m)

Figure 33.